JOURNAL OF PETROLOGY | VOLUME 42 | NUMBER 8 | PAGES 1519–1546 | 2001

Petrogenesis of the Labrieville Alkalic Anorthosite Massif, Grenville Province, Quebec

BRENT E. OWENS[1]* AND ROBERT F. DYMEK[2]

[1]DEPARTMENT OF GEOLOGY, PO BOX 8795, COLLEGE OF WILLIAM AND MARY, WILLIAMSBURG, VA 23187, USA
[2]DEPARTMENT OF EARTH AND PLANETARY SCIENCES, WASHINGTON UNIVERSITY, ST. LOUIS, MO 63130, USA

RECEIVED MARCH 21, 2000; REVISED TYPESCRIPT ACCEPTED FEBRUARY 12, 2001

*The Labrieville massif (~1010 Ma) is an eroded dome consisting of three zones: (1) a foliated inner core of pink anorthosite (~$An_{30}Or_{13}$, ~2100 ppm Sr, ~1300 ppm Ba) with minor leuconorite; (2) a foliated outer core of pink anorthosite (~$An_{35}Or_{10}$, ~1900 ppm Sr, ~850 ppm Ba) with more abundant leuconorite; (3) a border of foliated to massive green leucogabbro. Antiperthitic plagioclase, orthopyroxene, hemoilmenite, and small amounts of biotite are present in all rocks. The border zone contains additional clinopyroxene, magnetite, and apatite. Labrieville is more alkalic and Sr- and Ba-rich than almost all other massif anorthosites. The widespread presence of biotite and the high hematite content of hemoilmenite suggest crystallization from a relatively oxidizing and water-bearing magma. Collectively, these features imply that Labrieville originated from a magma that differed considerably from typical tholeiitic liquids. Major- and trace-element variations suggest that all rock types represent mixtures of cumulus minerals, with negligible trapped melt. The compositionally distinct zones imply differentiation during crystallization. Although plagioclase compositions become more evolved inward, other indicators (*e.g. X_{Mg} *in pyroxene) suggest differentiation outward from core to border. We favor the latter interpretation, and suggest that the increase in plagioclase An content reflects a decline in pressure during crystallization.*

KEY WORDS: *anorthosite; Grenville Province; plagioclase; cumulate processes*

INTRODUCTION

Massif anorthosites are an unique type of plutonic igneous rock consisting predominantly of a single mineral—plagioclase feldspar. The circumstances whereby such nearly monomineralic plutons can be produced have puzzled geologists for more than a century, and massif anorthosites remain petrologic enigmas. In addition to this fundamental aspect of the 'anorthosite problem' (see Bowen, 1917; Scoates, 2000), the petrogenesis of massif anorthosites was apparently restricted in time and space. Specifically, virtually all of the world's supply of massif anorthosite was formed during the Proterozoic, and much of it is found in the Grenville Province of Quebec and Labrador (Kranck, 1961; Anderson, 1969; Ashwal, 1993).

Despite their similar plagioclase-rich nature, it is now apparent that massif anorthosites worldwide are mineralogically and compositionally diverse (see Xue & Morse, 1993), implying involvement of a wide range of parental magma compositions or petrogenetic processes in their formation. However, comprehensive studies on individual anorthosite complexes that can elucidate their petrogenesis—combining field and petrographic observations with mineral-chemical data, and with complete major- and trace-element data on a wide range of rock types—are few in number. Admittedly, the immense size of certain massifs (e.g. Lac St. Jean Complex, Woussen *et al.*, 1988) and the remote or inhospitable locations of others (e.g. Kunene Complex, Angola, Ashwal & Twist, 1994; Nain Complex, Labrador, Ranson, 1981), plus the fact that many (perhaps most) large anorthosite bodies are composite in nature (e.g. Harp Lake, Labrador, Emslie, 1980), make investigations of the sort outlined above a challenging and long-term task. For example, the Laramie anorthosite complex, Wyoming, has been

*Corresponding author. Telephone: 757-221-1813.
e-mail: beowen@wm.edu

studied by numerous investigators over a period of many years (e.g. Fuhrman *et al.*, 1988; Kolker *et al.*, 1990; Frost *et al.*, 1993; Mitchell *et al.*, 1996; Scoates *et al.*, 1996; Scoates, 2000).

In contrast, the Labrieville, Quebec, massif anorthosite is ideal for detailed study on a somewhat shorter time scale because, at $\sim$300 km^2, it is one of the smaller massifs in the Grenville Province. Despite its small size, however, Labrieville is highly relevant to massif anorthosite petrogenesis because it contains virtually all of the rock types associated with anorthosite suites that have intrigued investigators for generations. Moreover, the young age for Labrieville ($\sim$1010 Ma; Owens *et al.*, 1994) sets it apart as one of several late- to post-tectonic anorthosites with respect to the Grenville orogeny. Therefore, interpretation of petrologic data is not complicated by the effects of Grenvillian metamorphism.

This paper has three broad objectives. First, we use spatial variations in mineral and rock compositions to address internal differentiation of the Labrieville massif and show that it is a concentrically zoned pluton. Second, we use variations in whole-rock compositions to evaluate the origin of the principal Labrieville rock types (anorthosite, leuconorite, leucogabbro) and show that they represent mixtures of cumulus crystals with little to no trapped liquid. In doing so, we outline a general strategy for the evaluation of whole-rock geochemical data on plagioclase-rich rocks of seemingly monotonous character. Third, we show by comparison with other plutons that Labrieville represents a compositional extreme among massif anorthosites.

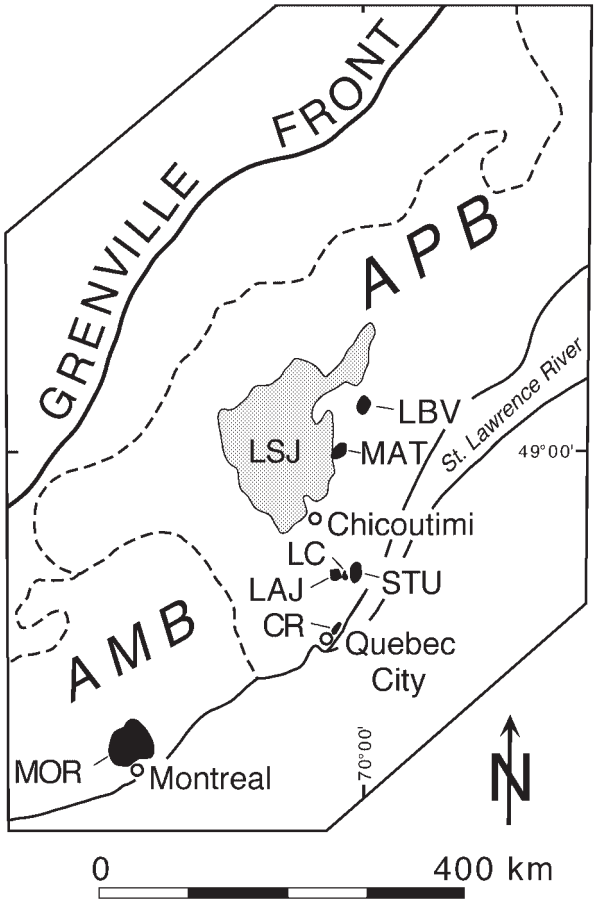

Fig. 1. Sketch map of the central Grenville Province showing the locations of the Labrieville (LBV), Mattawa (MAT), Lac à Jack (LAJ), Lac Chaudiere (LC), St. Urbain (STU), Château-Richer (CR), Lac St. Jean (LSJ), and Morin (MOR) anorthosite massifs. APB, Allochthonous Polycyclic Belt; AMB, Allochthonous Monocyclic Belt of Rivers *et al.* (1989).

REGIONAL SETTING

The Labrieville region (Fig. 1), situated in south–central Quebec $\sim$325 km NE of Quebec City, occurs in the Grenville Structural Province, within what has been termed the Central Granulite Terrain (Wynne-Edwards, 1972), the Core Zone (Woussen *et al.*, 1986), and the Allochthonous Polycyclic Belt (Rivers *et al.*, 1989). These names reflect the fact that Labrieville occurs in a segment of Grenville Province that experienced a protracted tectonothermal history from mid- to late Proterozoic times, highlighted by at least two episodes of anorthositic plutonism: emplacement of the Lac St. Jean massif at $\sim$1150 Ma (Higgins & van Breemen, 1992) and the Labrieville massif at $\sim$1010 Ma (Owens *et al.*, 1994). Elsewhere in the Allochthonous Polycyclic Belt, a third period of anorthositic magmatism occurred at $\sim$1060 Ma (Higgins & van Breemen, 1996). In fact, a semi-continuous belt of andesine anorthosites that post-date emplacement of the Lac St. Jean massif occurs in this region of Quebec, including the Château-Richer, St. Urbain, Lac Chaudiere, Lac à Jack, Mattawa, and Labrieville massifs (Fig. 1; Dymek & Owens, 1998*b*). Additional information on regional geology and geochronology has been given by Owens *et al.* (1994) and is not repeated here.

FIELD RELATIONS AND DESCRIPTIONS OF UNITS

Nomenclature

For purposes of description and discussion in this paper, the anorthositic rocks at Labrieville have been named on the basis of the amount of normative feldspar and the dominant ferromagnesian mineral(s) present. As illustrated in Fig. 2, the analyzed samples are all very rich in feldspar, whose normative composition ranges from $\sim An_{28}$ to $\sim An_{40}$. Rocks with >95% normative feldspar are termed 'anorthosite' (symbol A). Rocks with <95%

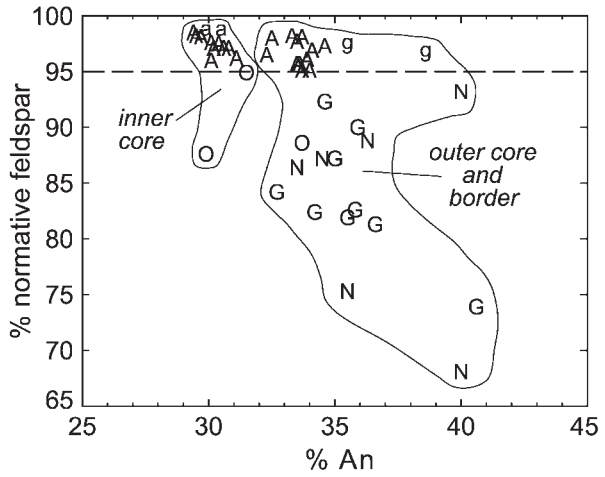

Fig. 2. Normative An vs normative feldspar for whole-rock samples of this study. (Note the abundance of rocks with >95% feldspar and the relatively sodic compositions.) A, anorthosite; N, leuconorite; G, leucogabbro; O, oxide anorthosite; a, plagioclase megacryst in core anorthosite; g, plagioclase megacryst in border leucogabbro.

feldspar are termed 'leuconorite' (symbol N) or 'oxide-anorthosite' (symbol O) based on whether the dominant mafic mineral is orthopyroxene or hemoilmenite (an exsolution intergrowth of hematite in ilmenite), respectively. Rocks with <95% feldspar that contain additional clinopyroxene are termed 'leucogabbro' (symbol G). We recognize that our usage of the term 'anorthosite' is more restrictive than in the IUGS classification scheme, which defines anorthosite as any rock with $\geq 90\%$ plagioclase. However, one of the principal features of Labrieville (and the other Quebec andesine anorthosites noted above) is the abundance and widespread presence of essentially 'pure-plagioclase' rocks, and one goal of our work was to investigate compositional changes accompanying the addition of other minerals to such rocks.

Almost without exception, the rock types correspond to the geographical distribution of the samples, with anorthosite, leuconorite, and oxide-anorthosite being found primarily in the core of the massif and leucogabbro in the border zone (see below). Also included in many figures are data points for plagioclase megacrysts (analyzed as whole-rock samples), both from core anorthosite (symbol a) and from border leucogabbro (symbol g). The locations of all samples for which data appear are shown in the sketch map of Fig. 3b.

Geological overview

As mapped by Anderson (1962, 1963, 1966), the Labrieville massif (Fig. 3a) comprises two structural domains: (1) a northern segment, which represents an eroded dome, consisting of a core of foliated anorthosite and leuconorite (plus a small hemoilmenite ore body), and a continuous border consisting of weakly foliated leucogabbro; (2) a southern segment called the Sault aux Cochons complex, which was interpreted by Anderson (1966) as a funnel-shaped intrusion, consisting of massive leucogabbro to mangerite [nomenclature revised from Anderson (1966)]. The present study deals entirely with the northern, 'anorthositic' segment. On the basis of regional correlations and distinctive patterns on aeromagnetic maps, we now believe that the Sault aux Cochons Complex represents a separate intrusion much like the nearby Lac Gouin Complex (see Hocq, 1977).

Core zones

On the basis of chemical compositions, the core zone can be divided into an inner [low An/(An + Ab)] and an outer region (Fig. 2), and an approximate boundary between them is shown in Fig. 3b. This separation of the core into two regions is not manifested in any obvious way through field or petrographic characteristics.

The predominant rock type in the core is anorthosite as defined above (Fig. 2). This anorthosite displays a seriate porphyritic texture consisting of a few percent blue–gray plagioclase megacrysts (from a few centimeters to $\sim$50 cm) set in a matrix of finer-grained ($\sim$1–10 mm), pink to brown plagioclase. Megacrysts range from tabular to blocky, and many contain Carlsbad and albite twins that can be observed with the naked eye.

Leuconorite is distributed irregularly throughout the core, with the best exposures found in the outer portion. Leuconorite occurs in banded sequences in which layers (from <1 m to several meters) containing plagioclase and medium- to coarse-grained orthopyroxene [in many cases as centimeter-sized megacrysts containing plagioclase exsolution lamellae (see Owens & Dymek, 1995)] alternate with anorthosite (Fig. 4a). Leuconorite also occurs as small 'patches' that weather preferentially, forming elongate depressions as a result (Fig. 4b). These patches are massive, range in size from a few centimeters to several decimeters, and appear to be somewhat disk-shaped (flattened) in three dimensions. They contain abundant fine- to medium-grained orthopyroxene crystals, which are possibly oikocrysts.

Most outcrops of core rocks display a prominent foliation—used here in a general sense for a planar rock fabric (Fig. 4a and b). This foliation is defined by: (1) discontinuous (centimeter- to decimeter-scale) layers of orthopyroxene, including pyroxene megacrysts; (2) thin (millimeter-scale) laminae of orthopyroxene and locally biotite; (3) the disk-shaped leuconorite depressions noted above; (4) the orientation of elongate plagioclase megacrysts. Attitudes on this foliation (Anderson, 1962, 1966; Morin, 1969; this study) show the massif to have a dome shape, in which dips increase from near horizontal in

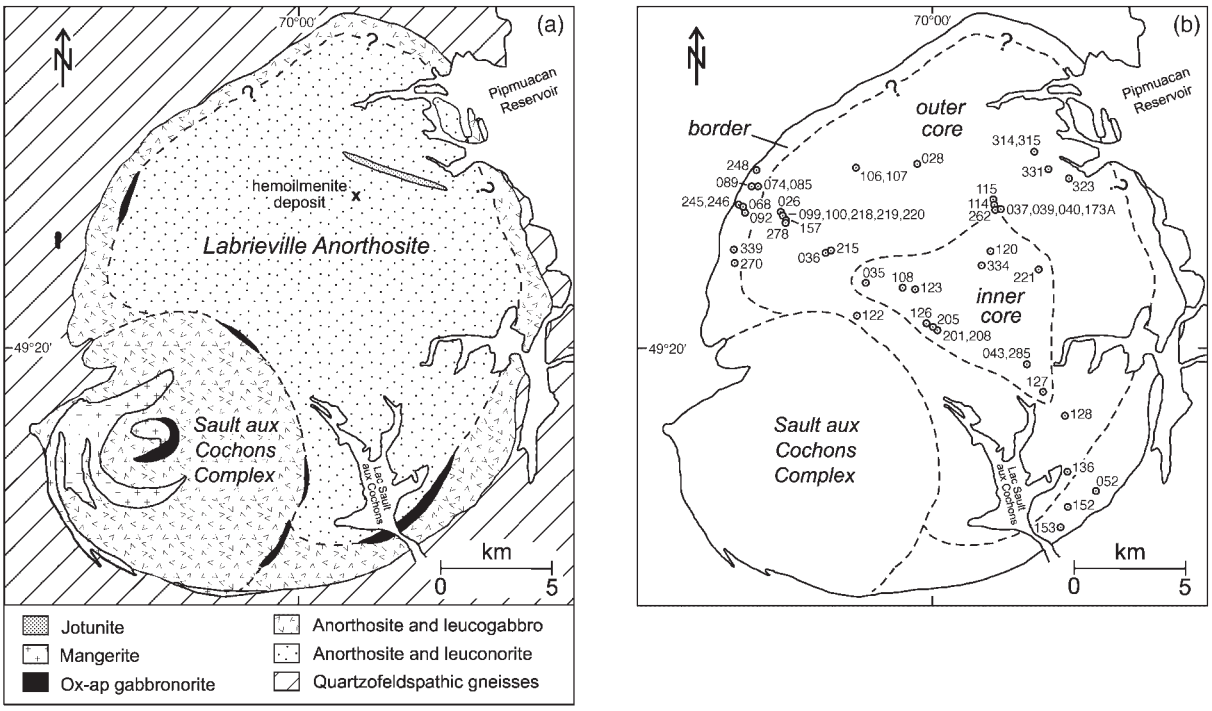

Fig. 3. (a) Geological sketch map of the Labrieville massif (adapted from Anderson, 1966); leucogabbro is present in both the border zone of the anorthosite and the Sault aux Cochons Complex, but the latter appears to be a separate intrusion. (b) Sample locations. [Note the separation of the leucogabbro border zone from a core zone of anorthosite–leuconorite. Note also the division of the core zone into inner and outer regions based on whole-rock compositions (see text for discussion).]

the interior to as much as 60° near the margins. The origin of this foliation is uncertain, but several other Grenville massifs also have dome shapes, and the doming has been attributed to diapiric rise of anorthosite (Martignole & Schrijver, 1970; see also Scoates, 2000).

Small amounts (<1%) of Fe–Ti oxide (hemoilmenite) occur in virtually every sample of anorthosite and leuconorite. Locally, however, certain outcrop areas contain higher proportions (up to 15%) of hemoilmenite, and these have been classified as oxide-anorthosite. The hemoilmenite forms irregularly shaped masses of variable size (from <1 cm to several meters across) and some could represent the recrystallized remnants of much larger crystals. These masses are more abundant in the vicinity of the Lac Brulé ore deposit (Fig. 4c; see below). Some oxide masses contain small (a few centimeters across) inclusions of anorthosite, and possess lobate-shaped reentrants that are suggestive of intrusive 'blobs' of an immiscible oxide melt.

The hemoilmenite deposit near Lac Brulé (Morin, 1969) crops out along a discontinuous series of narrow ridges (<30 m wide, oriented ~N10W) that extend for ~1 km. Contacts with enclosing anorthosite are poorly exposed (the deposit has not been mined), but are apparently sharp. Capping the ridges locally is a nelsonite horizon (hemoilmenite–apatite rock) up to 2 m thick (Dymek & Owens, 1996). This nelsonite is medium to coarse grained (≤5 mm), crudely banded, and contains up to 5% sulfide (predominantly pyrite) and rare corundum.

Border zone

The border zone of the massif ranges in width from <1 km near the western margin to ~2 km near the southeastern margin. It appears to be absent from the northern part of the intrusion, although Anderson (1966) inferred its presence around the entire periphery of the dome. In many places, the transition from core to border coincides with lenses of oxide–apatite gabbronorite (OAGN; Anderson, 1966; Owens & Dymek, 1992).

The border unit is variable in grain size and texture. In many places it is prominently foliated like the core, but locally it is very coarse grained and massive. This massive variety has been observed only near the western margin.

We have assigned the name 'leucogabbro' to the border zone to indicate the presence of clinopyroxene in addition to orthopyroxene in the mafic mineral assemblage. In addition, several other features distinguish the border zone from the core. First, although anorthosite is present

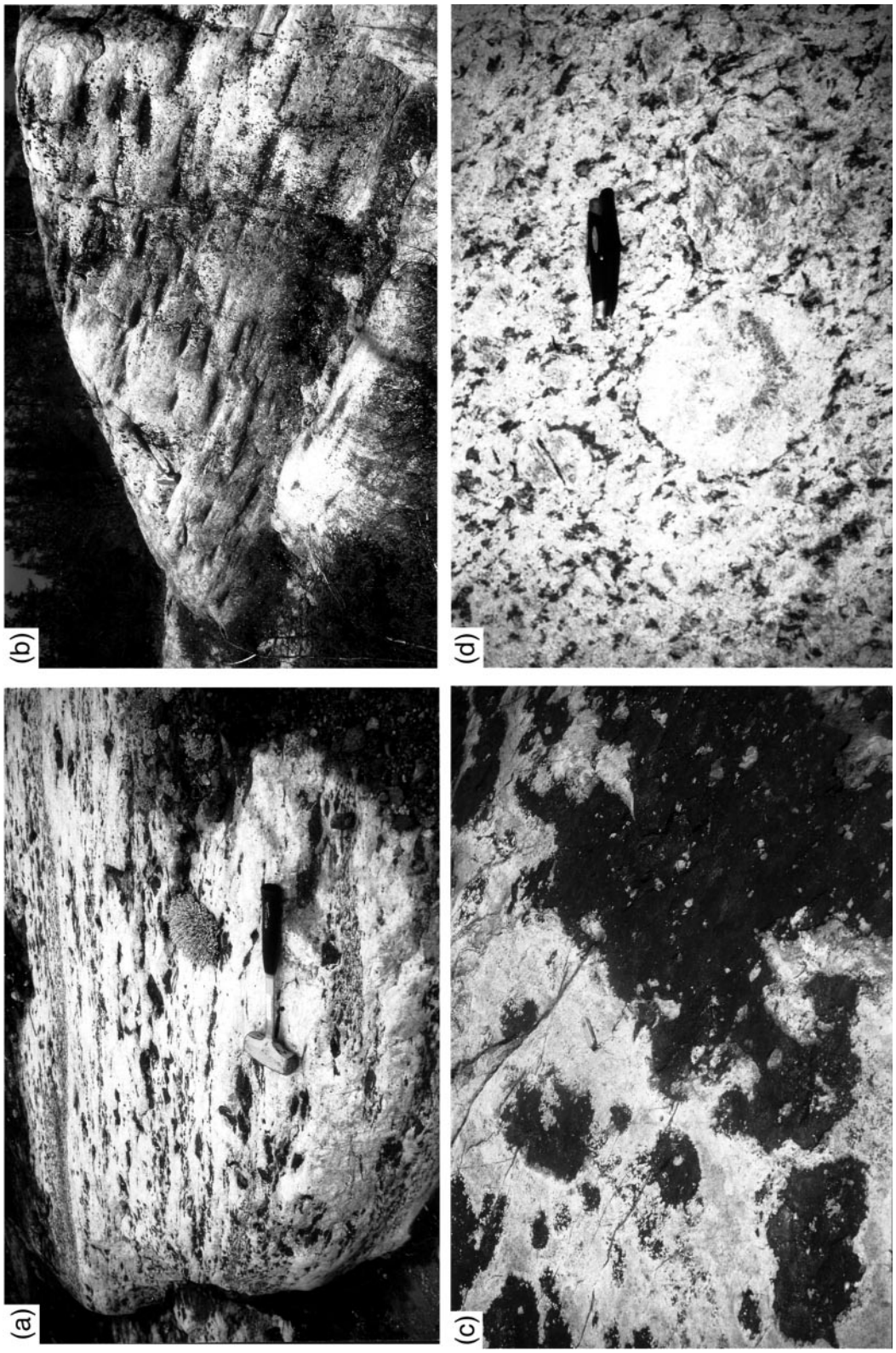

Fig. 4. Outcrop photographs of Labrieville rocks: (a) alternating layers of leuconorite and anorthosite; (b) foliation in core anorthosite–leuconorite defined by elongate depressions; (c) irregularly shaped masses of hemoilmenite in anorthosite; knife for scale in upper middle of photo; (d) massive border leucogabbro with plagioclase megacryst.

throughout, the border zone is everywhere more mafic than the core. Second, plagioclase megacrysts (~2–10 cm across) in border-zone rocks tend to be equant (Fig. 4d), in contrast to the more tabular shapes found in core-zone rocks. In a few places along the western margin, entire layers (up to ~10 m thick) consist almost entirely of these equant megacrysts. Third, the border zone contains magnetite, which is lacking in the core, in addition to hemoilmenite. Fourth, in contrast to the pink to brown color of the core-zone rocks, those in the border zone are generally green or gray–green. The reason for this color difference is not apparent. It may reflect a higher proportion of mafic minerals (some of which are altered) but even samples of anorthosite in the border are green. It is conceivable that this color difference is related to differences in oxidation state during crystallization of the two zones, with the pink core reflecting more oxidizing conditions.

PETROGRAPHY AND MINERAL COMPOSITIONS

The contrasting mineralogy of core and border zones is reflected in modal analyses of representative samples of two core-zone leuconorites (samples 099 and 218) and two border-zone leucogabbros (samples 092 and 152), which are listed in Table 1. The leuconorites and the leucogabbros are highly variable on the outcrop and hand-sample scale, and these modes (based on point counts of four thin sections from each sample) should be considered only as a rough indication of the proportions of minerals. The high cpx/opx ratio of the border zone (Table 1) compared with the core zone is a robust difference. Many rocks of the border zone are more altered than those of the core, as manifested by sericitized plagioclase, interstitial carbonate and quartz, minor chlorite, and uralitization of pyroxene.

Plagioclase grains in all rocks are anhedral, with highly irregular grain boundaries, and generally show no preferred orientation. Evidence for deformation appears as bent albite twin lamellae and the local development of subgrains. This deformation is not penetrative, and furthermore, there is no indication of extensive static recrystallization in these rocks.

Invariably, the plagioclase is antiperthitic, in which exsolved K-feldspar appears as small (<0·2 mm) blebs irregularly distributed throughout the host. K-feldspar also is found locally as small grains (<0·1 mm) interstitial to plagioclase, which probably represent products of 'granule' exsolution. Minute (<0·05 mm) grains of (exsolved?) hemoilmenite also occur in most plagioclase crystals. The abundance of these oxide blebs seems to be greater in plagioclase megacrysts than in matrix plagioclase.

Table 1: Modal mineralogy of leuconorites (N) and leucogabbros (G)

Sample:	099*	218†	092	152
Rock type:	N	N	G	G
Plagioclase‡	75·1	89·6	81·8	84·4
Quartz	0·1	0·1	0·4	1·2
Orthopyroxene	20·8	5·7	6·8	9·7§
Clinopyroxene	0·6	0·5	5·2	—
Biotite	1·2	0·1	tr	1·4
Hornblende	0·1	tr	—	tr
Ilmenite	1·2	3·6	3·2	1·1
Magnetite	—	—	0·8	0·4
Apatite	0·8	0·1	1·6	1·2
Sulfide	0·1	0·3	0·2	0·3
Calcite	—	—	—	0·3
Total points¶	5390	9167	4978	5453

*Leuconorite with orthopyroxene megacrysts.
†Medium-grained leuconorite.
‡Includes exsolved K-feldspar.
§Opx and cpx not distinguished because of alteration.
¶Counted on four thin sections of each sample.
tr, observed but not counted.

Plagioclase compositions range from An_{31} to An_{42}, with a peak at $An_{35–36}$ (Table 2). There is considerable overlap in composition between analyses from the core and border zones. As such, plagioclase An contents determined through spot analysis with the electron microprobe (EMP) do not clearly discriminate between these two main parts of the massif. For the most part, the compositions reported above are of grain interiors, and little zoning was detected at rims adjacent to other plagioclase grains. However, some of the more calcic compositions are of rims adjacent to mafic minerals, i.e. many plagioclase grains are reversely zoned. This feature also has been documented in the St. Urbain and Lac St. Jean anorthosites (Dymek, 1981; Woussen *et al.*, 1988) and in the Kiglapait layered intrusion, Labrador (Morse & Nolan, 1984), and may be a common feature of plagioclase-rich cumulates.

A few analyses of K-feldspar blebs from antiperthite are also listed in Table 2, and the compositions of these blebs along with corresponding hosts are illustrated on a ternary An–Ab–Or plot in Fig. 5a. The K-feldspar blebs approach pure end-member composition, with only a small amount of Na (<0·5 wt % Na_2O) and virtually no Ca, but they contain a high content of Ba (up to ~2 wt % BaO), which corresponds to as much as 5 mol % celsian ($BaAl_2Si_2O_8$).

Bulk compositions of plagioclase megacrysts from anorthosite and leucogabbro, plus normative compositions of

Table 2: Representative compositions of plagioclase and K-feldspar in Labrieville antiperthite

Sample:	208	201	106	106	036	036	092	092	152	106	122	092
Mineral:	plag	plag	plag	plag	plag	plag	plag	plag	plag	kspar	kspar	kspar
Rock type:	A-IC	N-IC	A-OC	A-OC	N-OC	N-OC	G	G	G	A-OC	A-OC	G
Comments:	core	core	core	rim-cpx	core	rim	core	rim-opx				
SiO_2	59·69	59·51	58·78	57·25	59·33	58·71	59·62	57·51	58·91	62·79	64·01	62·97
Al_2O_3	25·97	25·69	25·65	26·75	25·61	26·00	25·62	27·16	25·95	19·14	19·32	18·78
FeO	0·15	0·10	0·16	0·22	0·10	0·13	0·09	0·24	0·13	0·03	0·00	0·05
CaO	6·89	6·96	7·09	8·26	7·05	7·25	6·79	8·03	6·95	0·02	0·00	0·04
Na_2O	7·41	7·16	7·18	6·55	7·20	7·35	7·41	6·75	7·34	0·35	0·42	0·29
K_2O	0·46	0·59	0·53	0·45	0·39	0·41	0·42	0·38	0·37	16·17	15·79	16·14
BaO	0·03	0·03	0·00	0·00	0·00	0·00	0·00	0·00	0·02	1·27	0·45	1·35
Total	100·60	100·04	99·39	99·48	99·68	99·85	99·95	100·07	99·67	99·77	99·99	99·62
Formula proportions based on 8 oxygen atoms												
Si	2·649	2·655	2·643	2·581	2·655	2·629	2·660	2·576	2·639	2·944	2·963	2·958
Al	1·358	1·351	1·359	1·421	1·350	1·372	1·347	1·434	1·370	1·058	1·054	1·040
Fe	0·006	0·004	0·006	0·008	0·004	0·005	0·003	0·009	0·005	0·001	0·000	0·002
Ca	0·328	0·333	0·342	0·399	0·338	0·348	0·325	0·385	0·334	0·001	0·000	0·002
Na	0·638	0·619	0·626	0·573	0·625	0·638	0·641	0·586	0·637	0·032	0·038	0·026
K	0·026	0·034	0·030	0·026	0·022	0·023	0·024	0·022	0·021	0·967	0·932	0·967
Ba	0·001	0·001	0·000	0·000	0·000	0·000	0·000	0·000	0·000	0·023	0·008	0·025
Total	5·004	4·997	5·006	5·008	4·994	5·016	4·999	5·011	5·006	5·026	4·995	5·019
End-member proportions (mol %)												
An	33·0	33·7	34·2	40·0	34·3	34·5	32·8	38·8	33·6	0·1	0·0	0·2
Ab	64·3	62·8	62·7	57·4	63·4	63·2	64·8	59·0	64·2	3·1	3·9	2·6
Or	2·6	3·4	3·0	2·6	2·3	2·3	2·4	2·2	2·1	94·5	95·3	94·8
Cels	0·1	0·1	0·0	0·0	0·0	0·0	0·0	0·0	0·0	2·3	0·8	2·4

A-IC, anorthosite, inner core; A-OC, anorthosite, outer core; N-IC, leuconorite, inner core; N-OC, leuconorite, outer core; G, leucogabbro.

pure-plagioclase anorthosite are illustrated on a ternary An–Ab–Or plot in Fig. 5b. A comparison of these feldspar bulk compositions with the positions of isotherms on the ternary feldspar solvus (see Fuhrman & Lindsley, 1988) suggests a minimum temperature of crystallization >750°C, and some (perhaps all) crystallized at >900°C. Furthermore, comparison of Fig. 5a and b indicates that exsolution occurred at temperatures <750°C.

Orthopyroxene (pink–green pleochroic hypersthene) is the dominant mafic silicate throughout the core zone and typically occurs as equant to slightly elongate grains and grain clusters in the 0·5–2·0 mm size range. Nearly all grains contain abundant small exsolved platelets of hemoilmenite. Some grains contain fine-scale (100) exsolution lamellae of clinopyroxene, but most are free of such lamellae. There is no petrographic evidence for the former existence of pigeonite in any of the Labrieville rocks.

Small amounts of clinopyroxene (pale green salite) are also present in most core-zone rocks as small (~0·1 mm) interstitial grains or as thin (exsolved?) rims on orthopyroxene or Fe–Ti oxide; no exsolution features were observed in these grains. Larger (~1 mm) grains of clinopyroxene are common in border-zone leucogabbro. These grains typically contain very fine (100) exsolution lamellae of orthopyroxene.

Selected analyses of pyroxene from throughout the massif are listed in Table 3, and additional analyses have been given by Owens & Dymek (1995). Orthopyroxene compositions are in the range $En_{67–55}$ whereas clinopyroxenes are in the range $Ca_{48}Mg_{40}Fe_T+Mn_{12}$ to $Ca_{43}Mg_{37}Fe_T+Mn_{20}$. These compositions are relatively magnesian, given the alkalic nature of associated plagioclase. Thus, Labrieville lies at the extreme of the An–En paradox for massif anorthosites, first recognized by Anderson & Morin (1969). The paradox is that Labrieville

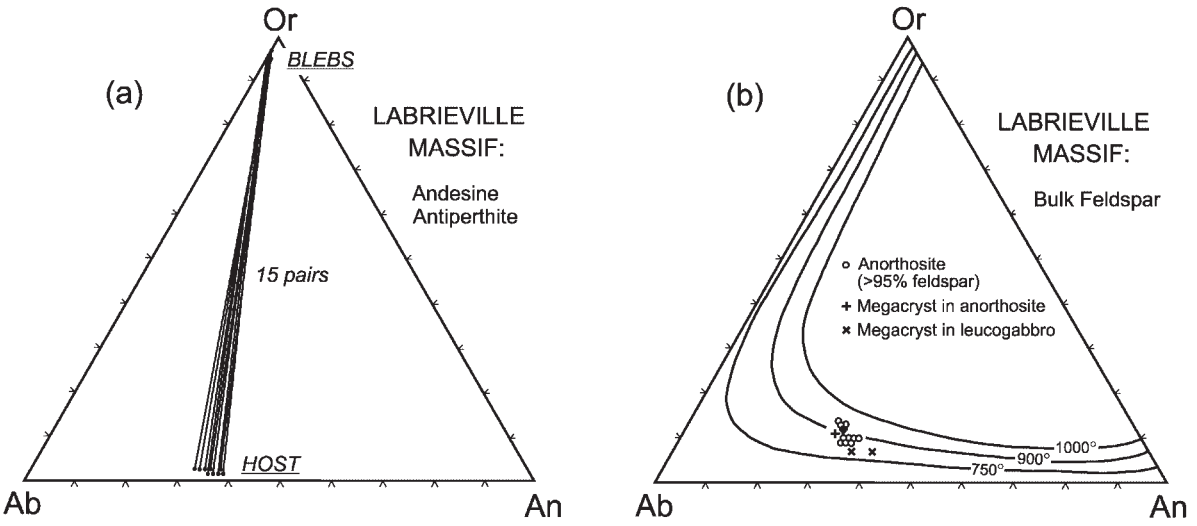

Fig. 5. Ternary plots of feldspar compositions. (a) Compositions of plagioclase hosts and K-feldspar blebs as determined by EMP analysis. (b) An–Ab–Or proportions of anorthositic whole rocks and plagioclase megacrysts as determined by XRF analysis. Isotherms (°C) on the ternary feldspar solvus are for reference only, and are adapted from Fuhrman & Lindsley (1988). Isotherms are drawn for 1 kbar (750°C, 1000°C) and 0·5 kbar (900°C), respectively.

and other massifs contain orthopyroxene that is much more magnesian at a given plagioclase An content than the compositions of such minerals in layered intrusions [see Fig. 10 below and discussion by Owens *et al.* (1993)]. Orthopyroxene contains small amounts of Al_2O_3 (1·0–1·5 wt %), TiO_2 (<0·1–0·2 wt %), MnO (0·3–0·7 wt %) and CaO (0·4–0·7 wt %), and negligible Na_2O (<0·05 wt %). Clinopyroxene contains higher amounts of Al_2O_3 (1·8–2·7 wt %), TiO_2 (0·2–0·5 wt %) and Na_2O (0·4–0·7 wt %), but lower MnO (0·1–0·4 wt %). Both pyroxenes contain negligible Cr_2O_3.

Values of X_{Mg} in pyroxene are illustrated in Fig. 6, which shows that pyroxenes from the border are slightly more Fe-rich than those from the core. Moreover, pyroxenes from the outer core range to more Fe-rich compositions than those from the inner core. Thus EMP spot analyses of pyroxene suggest a concentric progression in composition in the massif.

Hemoilmenite is the sole Fe–Ti oxide phase throughout the core zone, although some grains contain reduction lamellae of magnetite (see Anderson, 1966). The proportion of exsolved hematite lamellae is in the range of 20–40 vol. %. In many cases, multiple stages of exsolution are apparent, evidenced by a bimodal size distribution of hematite lamellae, in addition to small lamellae of ilmenite within larger lamellae of hematite. Magnetite in leucogabbro is typically free of exsolution features, but rare grains can be found with one or two ilmenite lamellae.

Representative compositions of Fe–Ti oxides are listed in Table 4. In hemoilmenite, the hosts are ferrian-ilmenite ($\sim Ilm_{65–75}$) and are enriched in Mg and Mn. The lamellae are titan-hematite ($\sim Ilm_{15–25}$), and are enriched in Al, V, and Cr. Magnetite in border leucogabbro contains small amounts of Al, V and Mn, and very low amounts of Ti; recalculated compositions indicate that most grains contain <0·5% of the ulvöspinel component.

The virtual absence of magnetite in the core rocks, together with the nearly end-member Fe_3O_4 composition of border-zone magnetite precludes the use of Fe–Ti oxide thermometry. However, a semi-quantitative indication of the temperature and oxygen fugacity conditions during crystallization can be inferred from the bulk composition of the hemoilmenite itself. In the system FeO–Fe_2O_3–TiO_2, the occurrence of a single oxide phase, in this case hemoilmenite, implies a specific relationship among composition, temperature, and oxygen fugacity. At a fixed temperature and Fe/Ti ratio, a higher fO_2 would result in the production of rutile (or possibly pseudobrookite) whereas a lower fO_2 would lead to the formation of magnetite. A higher fO_2 could produce a more hematite-rich ilmenite, but only if bulk Fe/Ti were to change.

X-ray fluorescence (XRF) analyses, obtained on several whole-rock samples of massive hemoilmenite (Table 5) were treated as equivalent to bulk-oxide compositions. The bulk composition of the Labrieville hemoilmenite ore is $\sim Ilm_{72}$, which is constrained to lie on an appropriate ilmenite isopleth in T–fO_2 space. This isopleth, as inferred from the results of Spencer & Lindsley (1981), lies between the hematite–magnetite (HM) and quartz–fayalite–magnetite (QFM) buffer curves. Thus, the crystallization conditions for the hemoilmenite deposit (and by inference the anorthosite massif), must have been a

Table 3: Representative compositions of pyroxene in various Labrieville rocks

Sample:	108	205	220	106	201	219	036	092	092	052	074
Mineral:	cpx	opx	opx	cpx	opx	opx	opx	opx	cpx	opx	opx
Rock type:	A-IC	A-IC	A-IC	A-OC	N-IC	N-OC	N-OC	G	G	G	G
SiO_2	51·34	52·15	51·58	51·37	53·18	52·09	52·43	50·81	50·81	51·21	50·64
TiO_2	0·30	0·13	0·06	0·36	0·11	0·13	0·08	0·12	0·27	0·13	0·14
Cr_2O_3	0·06	0·01	0·00	0·00	0·01	0·00	0·00	0·00	0·00	0·00	0·00
Al_2O_3	2·34	1·72	1·26	2·53	1·06	1·55	1·64	1·44	2·31	1·35	1·71
FeO	8·36	21·91	24·99	8·97	21·71	24·10	22·64	26·52	11·15	25·36	25·86
MnO	0·24	0·43	0·53	0·30	0·39	0·44	0·38	0·72	0·35	0·63	0·57
MgO	13·61	22·69	20·58	13·52	23·33	21·11	21·51	19·40	12·50	20·34	20·19
CaO	22·47	0·97	0·49	22·40	0·61	0·59	0·88	0·68	21·43	0·68	0·65
Na_2O	0·56	0·06	0·03	0·60	0·00	0·01	0·01	0·04	0·58	0·01	0·00
Total	99·28	100·07	99·52	100·05	100·40	100·02	99·57	99·73	99·40	99·71	99·76
Formula proportions based on 4 cations and 6 oxygen atoms											
Si	1·919	1·932	1·952	1·908	1·962	1·950	1·965	1·934	1·916	1·938	1·917
^{IV}Al	0·081	0·068	0·048	0·092	0·038	0·049	0·035	0·065	0·084	0·060	0·076
^{VI}Al	0·022	0·008	0·008	0·019	0·008	0·000	0·038	0·000	0·019	0·000	0·000
Cr	0·002	0·000	0·000	0·000	0·000	0·000	0·000	0·000	0·000	0·000	0·000
Fe^{3+}	0·081	0·057	0·039	0·096	0·024	0·049	0·000	0·064	0·092	0·056	0·075
Ti	0·008	0·004	0·002	0·010	0·003	0·001	0·002	0·003	0·008	0·004	0·004
Mg	0·758	1·253	1·161	0·748	1·283	1·248	1·202	1·100	0·703	1·147	1·139
Mn	0·008	0·013	0·017	0·009	0·012	0·013	0·012	0·023	0·011	0·020	0·018
Fe^{2+}	0·181	0·622	0·751	0·182	0·646	0·675	0·710	0·780	0·259	0·747	0·744
Ca	0·900	0·039	0·020	0·891	0·024	0·015	0·035	0·028	0·866	0·028	0·026
Na	0·041	0·004	0·002	0·043	0·000	0·001	0·001	0·003	0·042	0·001	0·000
End-member proportions (mol %)											
Ca	46·7	1·9	1·0	46·2	1·2	1·2	1·8	1·0	44·8	1·4	1·3
Mg	39·3	63·2	58·4	38·8	64·5	59·8	61·4	62·5	36·4	57·4	56·9
Fe(T) + Mn	14·0	34·9	40·6	14·9	34·3	39·0	36·8	36·5	18·8	41·2	41·8
X_{Mg}	0·744	0·649	0·595	0·729	0·657	0·610	0·629	0·566	0·666	0·588	0·582

few log units above QFM, and thus relatively oxidizing.

An important feature of the Labrieville rocks is the presence of biotite as an essential, nearly ubiquitous, minor phase. Biotite typically occurs in millimeter-sized, sheaf-like masses in association with orthopyroxene and/or hemoilmenite, and also as isolated grains interstitial to plagioclase. The biotite is typically brown or reddish brown, and a few EMP analyses reveal high contents of TiO_2 (~4–5 wt %), high X_{Mg} (~0·70–0·75), small amounts of F and negligible Cl. The common presence of biotite is a feature that Labrieville shares with the St. Urbain and several other Grenville massifs, suggesting that not all anorthosites are the products of exceptionally dry magmas.

Trace amounts of apatite (up to ~1·0 mm across) occur in numerous samples of core anorthosite and leuconorite, and apatite is an important constituent of nelsonite in the ore deposit. Apatite is considerably more abundant (up to ~2 modal %, Table 1) in border leucogabbro, and occurs in common association with pyroxene and Fe–Ti oxide.

Myrmekite occurs in minor amounts in numerous anorthosite samples along plagioclase–plagioclase grain boundaries or at the junction of several grains. Energy-dispersive analyses and back-scattered electron imaging reveal that they consist of calcic plagioclase (~$An_{60–70}$) plus quartz. As such, they appear similar in most respects to the calcic myrmekite described from the St. Urbain

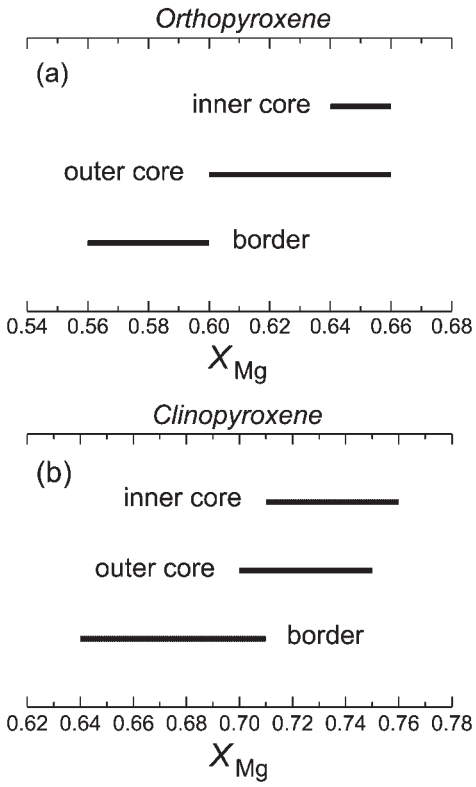

Fig. 6. One-way histograms illustrating variation in orthopyroxene (a) and clinopyroxene (b) X_{Mg} in rocks from the Labrieville massif. It should be noted that X_{Mg} decreases in the order inner core → outer core → border (see text for discussion).

anorthosite (Dymek & Schiffries, 1987), which has been interpreted as the product of late-stage aqueous corrosion of early formed plagioclase.

CHEMICAL COMPOSITIONS

Forty-four samples of anorthosite, leuconorite, oxide-anorthosite, and leucogabbro were analyzed for major and trace elements by XRF methods, and a subset of 23 samples was analyzed for additional trace elements by instrumental neutron activation analysis (INAA). Locations of these analyzed samples are shown in the sketch map of Fig. 3b, and selected analyses are listed in Table 6. The complete dataset is available by request from the authors.

Major elements

MgO was chosen as an index of variation because this oxide monitors the amount of non-plagioclase components in a given sample. This point is illustrated in Fig. 7, a plot of normative feldspar vs MgO. Here, data points for leuconorites and oxide-anorthosites form roughly linear arrays trending away from plagioclase, whereas leucogabbros define an intermediate array, reflecting the presence of both pyroxene and Fe–Ti oxide. The straightforward interpretation is that oxide-anorthosites, leuconorites, and leucogabbros represent mixtures of different mafic minerals with plagioclase, assembled in variable proportions.

The MgO-variation diagrams of Fig. 8 also illustrate the effects of mineral–mineral mixing in the Labrieville rocks. For example, although Al_2O_3 (Fig. 8a) varies essentially as a function of the amount of plagioclase, fields for oxide-anorthosite, leuconorite, and leucogabbro are distinct. In plots for Fe_2O_3-T and TiO_2 (Fig. 8b and c), the effect of adding pyroxene vs Fe–Ti oxide to plagioclase is readily apparent as leuconorites and oxide-anorthosites form distinct arrays, and the leucogabbros fall between these.

CaO in anorthosite ranges from 6 to 7 wt % (reflecting variable An in constituent plagioclase), but concentrations range to lower values for leuconorites and oxide anorthosites (Fig. 8d). Border leucogabbros, however, show an increase in CaO, which reflects mainly the added presence of clinopyroxene. Plagioclase megacrysts in leucogabbro are also higher in CaO (more anorthitic) than anorthosite in the core.

Na_2O (Fig. 8e) in anorthosite ranges from 6·0 to 6·5 wt % and mimics Al_2O_3. K_2O shows a wide range in anorthosite, from 1·5 to 2·3 wt %, and can be correlated crudely with percent normative feldspar (not plotted). K_2O decreases with the addition of other minerals, although it is also lower in plagioclase megacrysts from border leucogabbro than from anorthosite.

All core anorthosites and leuconorites contain very low P_2O_5 (typically <0·1 wt %; Fig. 8f). However, border leucogabbros typically contain higher amounts, up to 0·7 wt %, consistent with more abundant modal apatite.

Trace elements

Much of the variation in the analyzed rocks reflects the proportion of plagioclase in a given sample. For this reason, many of the figures dealing with trace elements contain two plots—one that shows the variation of the individual trace element with MgO, and a companion plot that illustrates how the various trace elements vary with respect to another element or oxide.

Sr, Ba, Rb

Strontium and Ba are the most abundant trace elements in the anorthositic rocks at Labrieville. Sr concentrations (Fig. 9a) are remarkably high, ranging from 1730 to 2270 ppm, apart from two samples with lower amounts (1243 and 1530 ppm), both of which come from near

Table 4: Representative compositions of Fe–Ti oxides in various Labrieville rocks

Sample:	037	037	106	106	092	092		092
Mineral:	ilm*	hem	ilm	hem	ilm	hem		mgt
Rock type:	ore	ore	A-OC	A-OC	G	G		G
MgO	2·30	0·70	0·52	0·22	0·40	0·13		0·03
Al_2O_3	0·03	0·10	0·01	0·13	0·03	0·14		0·66
SiO_2	0·02	0·01	0·02	0·01	0·00	0·00		0·03
TiO_2	48·12	18·10	47·07	15·88	48·22	15·92		0·00
V_2O_3	0·00	0·54	0·00	0·04	0·00	0·43		0·42
Cr_2O_3	0·02	0·11	0·00	0·02	0·00	0·00		0·19
MnO	0·25	0·04	1·50	0·07	0·64	0·05		0·19
FeO(T)	47·55	73·75	50·44	76·22	50·36	75·69		91·07
ZnO	0·00	0·00	0·00	0·00	0·00	0·00		0·00
Total	98·29	93·35	99·56	92·59	99·65	92·36		92·59
FeO†	38·94	15·00	39·90	13·83	42·00	14·03		30·74
Fe_2O_3†	9·57	65·29	11·71	69·34	9·29	68·52		67·04
Total	99·25	99·89	100·73	99·54	100·58	99·22		99·30
Formula proportions‡								
Si	0·001	0·000	0·001	0·000	0·000	0·000		0·001
Ti	0·909	0·354	0·889	0·313	0·912	0·315		0·000
Al	0·001	0·003	0·000	0·004	0·001	0·004		0·030
Cr	0·000	0·002	0·000	0·000	0·000	0·000		0·006
V	0·000	0·011	0·000	0·000	0·000	0·000		0·013
Fe^{3+}	0·181	1·276	0·221	1·368	0·176	1·357		1·949
Mg	0·086	0·027	0·020	0·009	0·015	0·005		0·002
Fe^{2+}	0·818	0·326	0·838	0·303	0·883	0·309		0·993
Mn	0·005	0·001	0·032	0·002	0·014	0·001		0·006
Zn	0·000	0·000	0·000	0·000	0·000	0·000		0·000
End-member proportions (mol %)								
Geik§	8·6	2·7	2·0	0·9	1·5	0·5	Spn	1·5
Pyr	0·5	0·1	3·2	0·2	1·4	0·1	Chr	0·3
Ilm	81·8	32·9	83·8	30·4	88·3	31·1	Usp	0·0
Hem	9·0	64·3	11·1	68·6	8·8	68·3	Mgt	98·2

*Ilm and hem refer to ilmenite host and hematite lamellae, respectively, in hemoilmenite.
†Calculated from stoichiometry.
‡Based on two cations and three oxygen atoms for ilmenite and hematite, three cations and four oxygen atoms for magnetite.
§End-member abbreviations: Geik, geikelite; Pyr, pyrophanite; Ilm, ilmenite; Hem, hematite; Spn, spinel; Chr, chromite; Usp, ulvöspinel; Mgt, magnetite.

the ore deposit (sample 040 is at the anorthosite–ore contact). The leuconorites and leucogabbros all contain less Sr, although the amounts are still high (~1200–1800 ppm). Strontium correlates very well with Na_2O (not plotted), reflecting a plagioclase dilution trend, but correlates poorly with CaO (Fig. 9b). The distribution of data points in Fig. 9b suggests mixing among orthopyroxene and ilmenite (which plot near the origin), plagioclase of variable composition, and clinopyroxene at higher CaO and lower Sr.

Concentrations of Ba are also very high, and span a range in anorthosite from 670 to 1250 ppm. Levels of Ba in leuconorites, oxide-anorthosites, and leucogabbros are also high, but show no correlation with MgO (Fig. 9c), in contrast to Sr. The range of Ba concentrations appears to be controlled primarily by the amount of K_2O (Fig. 9d).

Concentrations of Rb (~3–12 ppm) are uniformly low, despite the Na- and K-rich nature of this massif. For the sample set as a whole, Rb correlates poorly with

Table 5: Major element compositions of Labrieville massive hemoilmenite

Sample:*	039	114	315
SiO_2	0·30	0·42	0·07
TiO_2	36·57	36·66	36·56
Al_2O_3	1·48	1·74	0·52
Fe_2O_3(T)	61·28	61·02	63·30
MnO	0·14	0·13	0·18
MgO	2·12	2·35	1·74
CaO	0·15	0·15	0·04
Na_2O	0·01	0·10	0·20
K_2O	0·03	0·03	0·01
P_2O_5	0·01	0·01	0·00
LOI	−2·72	−2·95	−3·02
Total	99·43	99·66	99·60
Ilmenite†	72·2	72·4	70·7
Hematite	27·8	27·6	29·3

*Samples 039 and 114 are massive hemoilmenite from the ore deposit; sample 315 is an oxide segregation within anorthosite.
†End-members calculated by the method of Lindsley & Spencer (1982); ilmenite includes $MgTiO_3$ and Al_2O_3.

MgO but increases with K (not plotted). As a result of low Rb concentrations, K/Rb values are extremely high (all >1000, most >2000), whereas Rb/Sr values are all extremely low (<0·006).

Ga

Ga concentrations in anorthosite are relatively low (~19–24 ppm, Fig. 10a). Such low levels of Ga, coupled with high Al, result in values of Ga/Al that are much lower than those of plagioclase from basaltic rocks (see Dymek, 1990). In leuconorites, concentrations of Ga range to slightly lower values, probably reflecting 'dilution' by orthopyroxene, but values are slightly higher in leucogabbros, which is probably due to the presence of magnetite in those rocks. Contrary to general expectations (e.g. Goodman, 1972) Ga does not correlate with Al in this sample suite (not plotted).

Transition metals

Nickel shows an increase with MgO (Fig. 10b), and this is also the case for Sc, Cr, Co, and Zn (not plotted). Thus, leuconorites, oxide-anorthosites, and leucogabbros all contain higher amounts than anorthosite, confirming that pyroxene and hemoilmenite are both important reservoirs for these elements. However, the different rock types display contrasting positive correlations, reflecting both the type and modal abundance of the predominant mafic mineral (or minerals) present. For example, for a given MgO content, Ni is higher in leuconorites than in leucogabbros, but the reverse is true for V. The latter element correlates well with Ti (not plotted), indicating that V is harbored primarily in hemoilmenite. Values of Ti/V are high in all samples, in most cases >100, a feature that appears to be a characteristic of the anorthosite–jotunite–mangerite suite (see Owens *et al.*, 1993).

Zr, Hf, Y, Nb, Ta

Zirconium concentrations are low in anorthosite, with most samples having <20 ppm (Fig. 10d). Leuconorites show only slightly higher Zr, but oxide-anorthosites and leucogabbros contain up to 80 ppm. Zirconium and Ti correlate fairly well (not plotted), suggesting either that Zr is harbored in hemoilmenite, or that zircon is associated primarily with Fe–Ti oxide. Although there is some scatter, Zr and Hf are correlated positively (not plotted), as expected. Values of Y, Nb, and Ta are very low in all rocks (typically at or below the detection limit), although higher amounts of Ta (up to 0·4 ppm) are found in oxide-anorthosites and some leucogabbros.

Rare earth elements (REE)

A general indication of how the REE are distributed among the various lithologies can be gained through plots of La and Yb vs MgO. Figure 11a shows that anorthosites and oxide-anorthosites have La concentrations in the 2–4 ppm range. Lanthanum concentrations remain relatively constant as MgO increases in the leuconorites, although the leuconorites have slightly higher amounts than some anorthosites. Leucogabbros, on the other hand, have consistently higher amounts (~6–10 ppm). Lanthanum and P_2O_5 are positively correlated (Fig. 11b), albeit crudely, suggesting that apatite is the primary reservoir for the light REE (LREE), at least in rocks that contain more than ~4 ppm La.

In contrast to La, Yb and MgO are correlated positively in the leuconorites (Fig. 11c), reflecting the 'compatible' nature of Yb in orthopyroxene. Values of Yb are generally higher in the leucogabbros and show a crude positive correlation with P_2O_5 (Fig. 11d), suggesting that apatite (in addition to pyroxene) is an important reservoir for the heavy REE (HREE) in these rocks.

The concentrations of REE are illustrated further in a series of chondrite-normalized diagrams in Fig. 12. The LREE concentrations are low in anorthosite (La_N

Table 6: Selected whole-rock compositions of Labrieville anorthosites, oxide-anorthosites, leuconorites, and leucogabbros (major elements in wt %, trace elements in ppm)

Sample:	035	262	285	285p	106	122	136	108	126
Type:*	A-IC	A-IC	A-IC	a-IC	A-OC	A-OC	A-OC	O	O
SiO_2	58·8	59·7	59·3	59·3	59·0	59·0	58·4	57·9	52·5
TiO_2	0·38	0·08	0·19	0·12	0·12	0·15	0·12	1·21	4·67
Al_2O_3	23·5	23·8	23·6	24·1	24·5	24·3	24·4	23·1	20·9
Fe_2O_3(T)	1·11	0·47	0·66	0·56	0·49	0·67	0·77	2·84	8·62
MnO	0·02	0·01	0·01	0·01	0·01	0·00	0·01	0·02	0·04
MgO	0·0	0·0	0·0	0·1	0·0	0·0	0·1	0·1	0·4
CaO	6·12	6·13	6·10	6·26	6·84	6·75	6·81	6·25	5·32
Na_2O	6·24	6·35	6·29	6·41	6·34	6·41	6·18	6·11	5·46
K_2O	2·12	2·34	2·27	2·12	1·67	1·67	1·79	1·86	1·95
P_2O_5	0·07	0·07	0·03	0·05	0·06	0·03	0·04	0·06	0·08
LOI	0·34	0·22	0·24	0·21	0·21	0·17	0·37	0·33	0·03
Total	98·70	99·11	98·77	99·28	99·25	99·14	98·98	99·77	99·95
% Fsp†	97·5	98·5	98·1	98·9	98·2	98·0	98·1	94·9	87·6
% An	30·4	29·4	29·7	30·5	33·3	32·5	33·7	31·5	29·9
% Or	12·7	13·8	13·5	12·4	9·9	9·9	10·6	11·4	13·3
Sc	0·30	0·04	0·12	0·16	0·09	0·21	0·17	1·40	3·49
V	12·5	<10	<7	<10	<10	<10	<12	30·7	210
Cr	0·3	<0·2	0·8	0·2	0·5	0·3	0·2	15·3	27·0
Co	2·04	0·47	0·73	0·89	0·62	1·19	0·85	4·34	18·00
Ni	<5	<6	<6	<5	<10	<10	<5	<6·5	14·4
Cu	<8	<7	<6	<7	<7	<10	<7	<7	<9
Zn	5·1	<3	<4	<4	<4	4·3	5·6	14·0	13·9
Ga	20·8	21·1	21·0	20·5	20·2	20·9	20·7	20·6	23·1
As	<0·8	<0·3	<0·4	—	—	<0·3	<0·3	<0·7	<0·5
Br	0·52	0·32	0·79	0·88	0·39	0·39	0·48	0·73	0·43
Rb	5·1	7·3	7·1	5·2	3·7	5·7	6·3	6·4	6·8
Sr	2153	2085	2267	2252	2102	1996	1883	1759	1819
Y	<3	<2	<2	<2	<2	<2	<3	<3	<3
Zr	7·4	6·2	18·3	18·5	<4	9·2	27·7	31·3	72·4
Nb	<2	<2	<2	<2	<2	<2	<2	<3	3·0
Sb	<0·005	<0·005	<0·030	<0·005	<0·013	—	<0·006	<0·016	<0·030
Cs	<0·012	<0·020	0·010	<0·2	<0·020	0·014	0·044	0·021	<0·05
Ba	1217	1375	1424	1262	871	826	783	926	1099
La	3·25	2·51	2·20	2·80	2·16	2·56	3·66	4·09	2·70
Ce	5·93	4·27	3·87	5·08	3·83	4·58	6·54	7·33	4·85
Sm	0·439	0·220	0·199	0·346	0·223	0·319	0·444	0·489	0·362
Eu	0·964	1·008	0·918	0·946	0·751	0·796	0·918	1·065	0·911
Tb	0·031	0·011	0·010	0·027	0·012	0·027	0·034	0·034	0·026
Yb	0·040	<0·03	<0·03	0·027	—	0·028	0·036	0·074	0·050
Lu	<0·010	<0·005	<0·004	<0·009	<0·004	0·005	0·006	0·009	0·007
Hf	0·19	<0·05	0·04	0·10	0·06	0·17	0·23	0·84	1·82
Ta	0·04	<0·02	0·01	0·01	<0·02	0·01	0·01	0·14	0·30
W	<0·7	<0·7	<0·5	<0·6	<0·6	<0·4	<0·9	<2	<0·7
Pb	<5	5·9	5·7	<8	<9	<7	<7	<5·4	<9·4
Th	0·023	<0·013	<0·018	0·018	<0·021	<0·050	0·013	<0·030	0·028
U	<0·16	<0·16	<0·15	<0·12	—	<0·07	<0·13	<0·16	<0·20

Table 6: continued

Sample:	036	099	107	218	074	074p	089	153
Type:*	N	N	N	N	G	g	G	G
SiO_2	58·3	55·2	56·9	55·4	50·1	57·3	53·7	55·3
TiO_2	0·23	0·72	0·93	1·43	3·13	0·22	1·73	1·05
Al_2O_3	22·79	17·05	21·85	21·58	18·53	24·88	20·09	21·5
Fe_2O_3(T)	2·15	9·83	4·40	5·41	11·72	0·99	6·74	4·82
MnO	0·03	0·15	0·05	0·05	0·11	0·02	0·07	0·07
MgO	1·09	6·51	1·87	2·01	3·51	0·18	1·56	1·4
CaO	6·33	5·60	5·99	6·43	6·82	7·75	7·12	7·40
Na_2O	5·96	4·21	5·36	5·52	4·09	5·92	5·22	5·47
K_2O	1·80	1·02	1·62	1·32	1·01	1·19	1·47	1·25
P_2O_5	0·07	0·10	0·10	0·09	0·22	0·04	0·27	0·34
LOI	0·30	0·06	0·18	0·19	0·21	0·18	1·15	0·44
Total	99·04	100·40	99·29	99·44	99·43	98·63	99·12	99·09
% Fsp†	93·2	68·1	86·4	87·2	73·9	97·0	84·2	87·2
% An	40·0	40·0	33·5	34·5	40·6	38·6	32·7	35·0
% Or	11·3	8·8	11·0	8·9	8·3	7·2	10·5	8·5
Sc	1·79	9·72	3·08	3·82	7·40	0·32	8·10	n.d.
V	<14	51·2	46·2	65·4	188	<8	75·5	56·6
Cr	4·4	50·0	19·9	27·9	<3	0·3	2·3	n.d.
Co	8·33	39·2	17·7	20·8	44·5	1·79	16·6	n.d.
Ni	10·9	37·1	37·9	39·6	26·8	<6	<7	11·5
Cu	<15	<9	25·0	13·7	14·1	<7	<8	<6
Zn	18·4	112	33·5	39·3	110	7·6	51·4	43·4
Ga	19·9	19·3	20·3	22·5	25·2	19·4	26·0	22·2
As	<0·4	<4	<0·4	<0·4	—	<0·3	<0·6	n.d.
Br	0·26	<0·5	<0·4	<0·3	0·39	<0·3	<0·9	n.d.
Rb	6·0	3·3	5·7	5·6	2·6	4·0	6·3	3·5
Sr	1857	1212	1796	1661	1539	2173	1482	1774
Y	<3	5·3	<4	<4	7·8	<2	6·9	7·1
Zr	21·3	25·5	12·6	25·0	79·5	25·0	48·1	40·4
Nb	<2	<3	<2	<2	4·2	<2	2·8	<2
Sb	<0·006	<0·07	<0·03	<0·03	—	<0·006	<0·03	n.d.
Cs	<0·03	<0·10	<0·05	<0·07	<0·07	0·028	<0·06	n.d.
Ba	897	541	860	654	673	562	948	693
La	3·83	4·27	3·96	3·59	8·34	2·22	7·67	n.d.
Ce	7·41	8·92	8·16	6·96	18·8	4·57	17·0	n.d.
Sm	0·683	1·133	0·784	0·689	2·66	0·443	2·45	n.d.
Eu	0·958	0·904	0·926	0·871	1·52	1·123	1·72	n.d.
Tb	0·072	0·157	0·079	0·076	0·307	0·040	0·307	n.d.
Yb	0·117	0·530	0·158	0·179	0·590	0·057	0·590	n.d.
Lu	0·022	0·086	0·024	0·027	0·086	0·007	0·082	n.d.
Hf	0·35	0·78	0·46	0·76	2·24	0·21	1·26	n.d.
Ta	0·03	0·08	0·09	0·13	0·43	0·02	0·21	n.d.
W	<0·7	<0·6	<1·0	<0·7	<1·1	<0·6	<0·9	n.d.
Pb	<10	<8	5·0	5·2	<8	<6	<10	<9
Th	0·028	0·028	0·053	0·053	0·127	0·026	0·118	n.d.
U	<0·2	<0·2	<0·3	<0·15	<0·20	<0·17	<0·3	n.d.

—, below detection limit; n.d., not determined.
*Rock type designations as in Table 2, with additional 'a' and 'g', which are plagioclase megacrysts in anorthosite and leucogabbro, respectively.
†% Fsp = normative An + Ab + Or; % An = 100[An/(An + Ab + Or)]; % Or = 100[Or/(An + Ab + Or)].

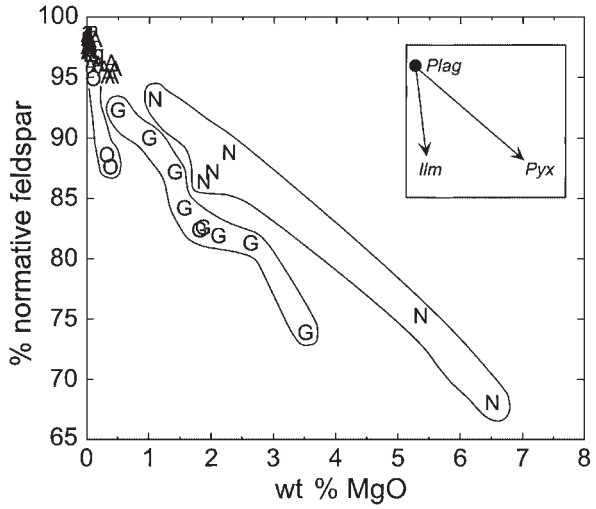

Fig. 7. Normative feldspar vs MgO in whole rocks. The inset shows the directions that data arrays would take for mixing of ilmenite or pyroxene to plagioclase (symbols as in Fig. 2).

~7–11 ×), and overall pattern shapes are steeply fractionated with large positive Eu anomalies (Fig. 12a). Concentrations of HREE are extremely low, and in some samples only maximum values could be estimated for Yb and Lu. Samples from the inner and outer core regions overlap with respect to REE concentrations. The chondrite-normalized patterns for the oxide anorthosites are essentially identical to those of the anorthosites (Fig. 12b). Leuconorites, in contrast, differ from anorthosites in containing slightly (La, Ce, Sm) to significantly (Tb, Yb, Lu) higher amounts of all REE except for Eu. Thus, chondrite-normalized pattern shapes for leuconorites are considerably less fractionated than those for anorthosites, and patterns become flatter as the total amount of REE increases (Fig. 12a). In addition, the magnitude of the positive Eu anomaly is diminished.

Concentrations of REE in one anorthosite and several leucogabbros from the border unit are illustrated in Fig. 12c. Anorthosite from the border is similar to some core anorthosites with respect to the LREE, but contains a higher concentration of HREE, such that its chondrite-normalized pattern is not as steeply fractionated. Leucogabbros tend to contain higher amounts of all REE than core anorthosites and leuconorites, and their pattern shapes do not show the flattening in the HREE of the leuconorites. Within the leucogabbros, the range in REE concentrations is not well correlated with MgO, but is more closely correlated with P_2O_5 (Fig. 11). As noted above, this observation suggests that the REE patterns of the leucogabbros do not primarily reflect the isolated effect of additional pyroxene (as is true for leuconorites), but rather show the combined effects of additional pyroxene plus apatite.

Concentrations of REE in two plagioclase megacrysts from core anorthosite and two from border leucogabbro are illustrated in Fig. 12d. Although their chondrite-normalized patterns are similar, megacrysts in leucogabbro have slightly lower La and Ce, but higher Sm, Eu, and HREE than those in core anorthosite. The net effect of these differences is that leucogabbro megacrysts display patterns that are rotated slightly in an anticlockwise direction relative to patterns for megacrysts in anorthosite.

DISCUSSION

Labrieville compositional extremes

Since the work of Anderson (1966), the Labrieville massif has been recognized as an alkalic, oxidized anorthosite, characterized by andesine–antiperthite and hemoilmenite. The results of the present study provide comprehensive and quantitative confirmation of these observations, and reveal unusually high concentrations of Sr and Ba in all rock types as well. To illustrate these compositional extremes, the Labrieville data are compared with results (also obtained in the Washington University laboratory) from two other Grenville anorthosites—the St. Urbain and Morin massifs.

Normative, whole-rock feldspar compositions of these anorthosites are illustrated in Fig. 13. There is a clear progression in normative An from Morin ($\sim An_{54–41}$) to St. Urbain ($\sim An_{46–36}$) to Labrieville. Furthermore, Labrieville is more potassic than the other massifs, ranging up to Or_{14}. These results confirm the highly alkalic nature of the Labrieville anorthosite, which is possibly surpassed only by the Roseland, Virginia, massif, for which preliminary results yield $\sim An_{29}Or_{16}$ (Owens & Dymek, 1999*a*). Compositions for other anorthosites (e.g. Nain, Adirondacks, Lac St. Jean) range to higher An than those considered here and are not plotted.

Normative feldspar compositions of whole-rock samples from the Kiglapait layered intrusion, Labrador (Morse, 1981) are included for comparison in Fig. 13. Feldspar compositions as potassic as those at Labrieville are not achieved until the upper part of the Upper Layered Zone, and at an even lower An content. The Kiglapait trend extends to even more evolved feldspars (mesoperthites; $\sim An_9Or_{33}$) at the top of the Upper Layered Zone (Fig. 13). Figure 13 also includes data from whole-rock samples from the Skaergaard layered intrusion, Greenland (McBirney, 1989). It can be seen on this plot that the Labrieville compositions are also more potassic, for a given An content, than late-stage Skaergaard feldspars, and several compositions have even higher normative Or than the most evolved feldspars in the Sandwich Horizon (Wager & Brown, 1967). An additional observation is that the feldspars of all three

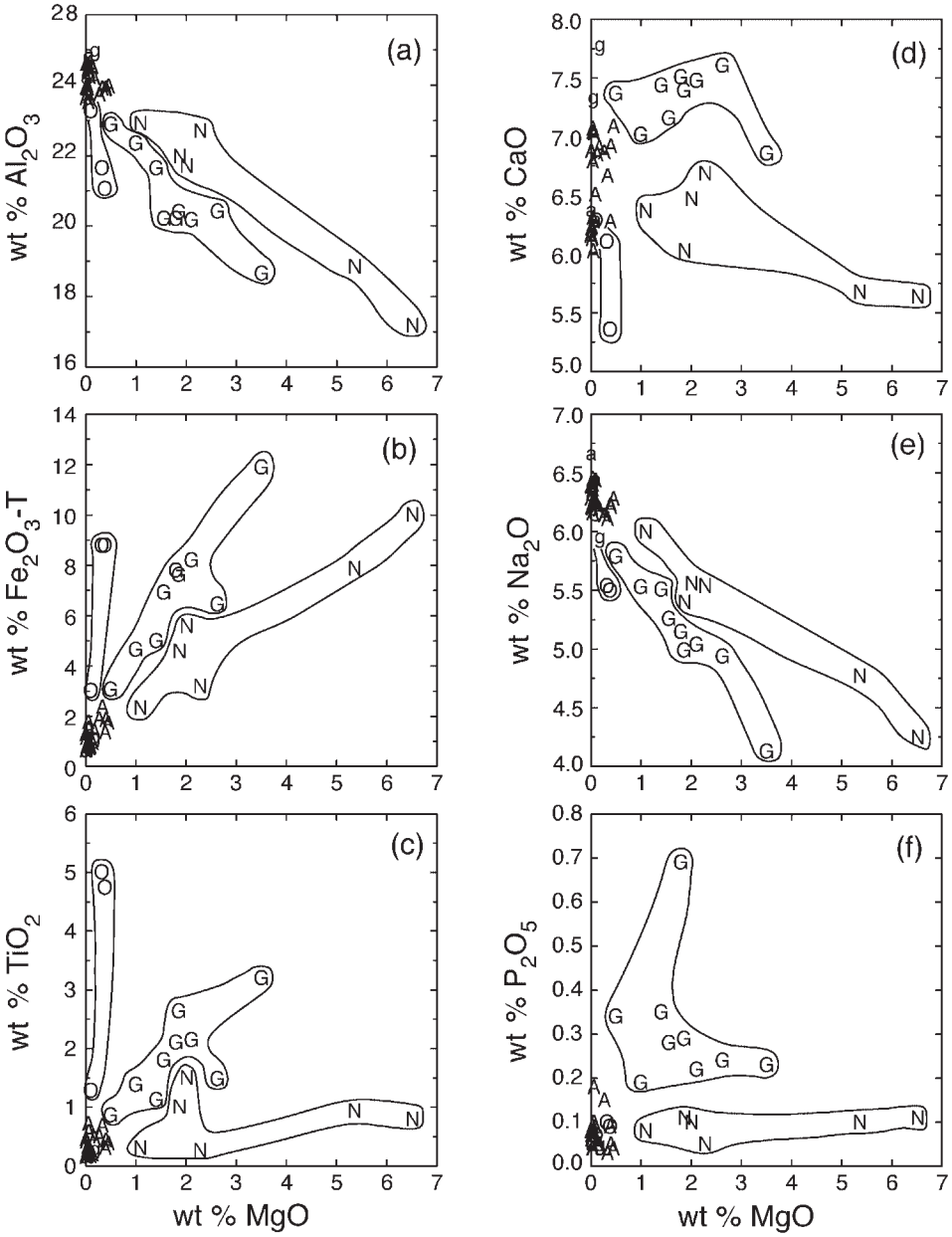

Fig. 8. Major-element, MgO-variation diagrams for rocks of the Labrieville massif (symbols as in Fig. 2). Symbols for anorthosites and plagioclase megacrysts show considerable overlap in this and some subsequent figures, but in no case are symbols for leuconorites and leucogabbros obscured by the anorthosite cluster.

massifs (at a given An content) are more potassic than those from the Kiglapait and Skaergaard intrusions.

One possible explanation for the alkalic nature of Labrieville feldspars is that they represent highly evolved compositions analogous to those formed at the last stages of differentiation of Skaergaard- or Kiglapait-type liquids. For the Skaergaard or Kiglapait intrusions, the evolved character of their late-stage feldspars can be attributed to extensive and prolonged prior fractionation of plagioclase. At Labrieville, however, there is no field evidence for the existence of the substantial volume of earlier-formed, more calcic plagioclase required by such a model. Furthermore, the extreme levels of Sr in Labrieville plagioclase preclude any significant prior plagioclase fractionation in the history of this massif (unless accompanied by the fractionation of prodigious quantities of low-Sr mafic phases, for which there is also no evidence). For the same reason, the progression in plagioclase compositions from Morin to St. Urbain to Labrieville cannot be interpreted as a fractionation trend, because the absolute

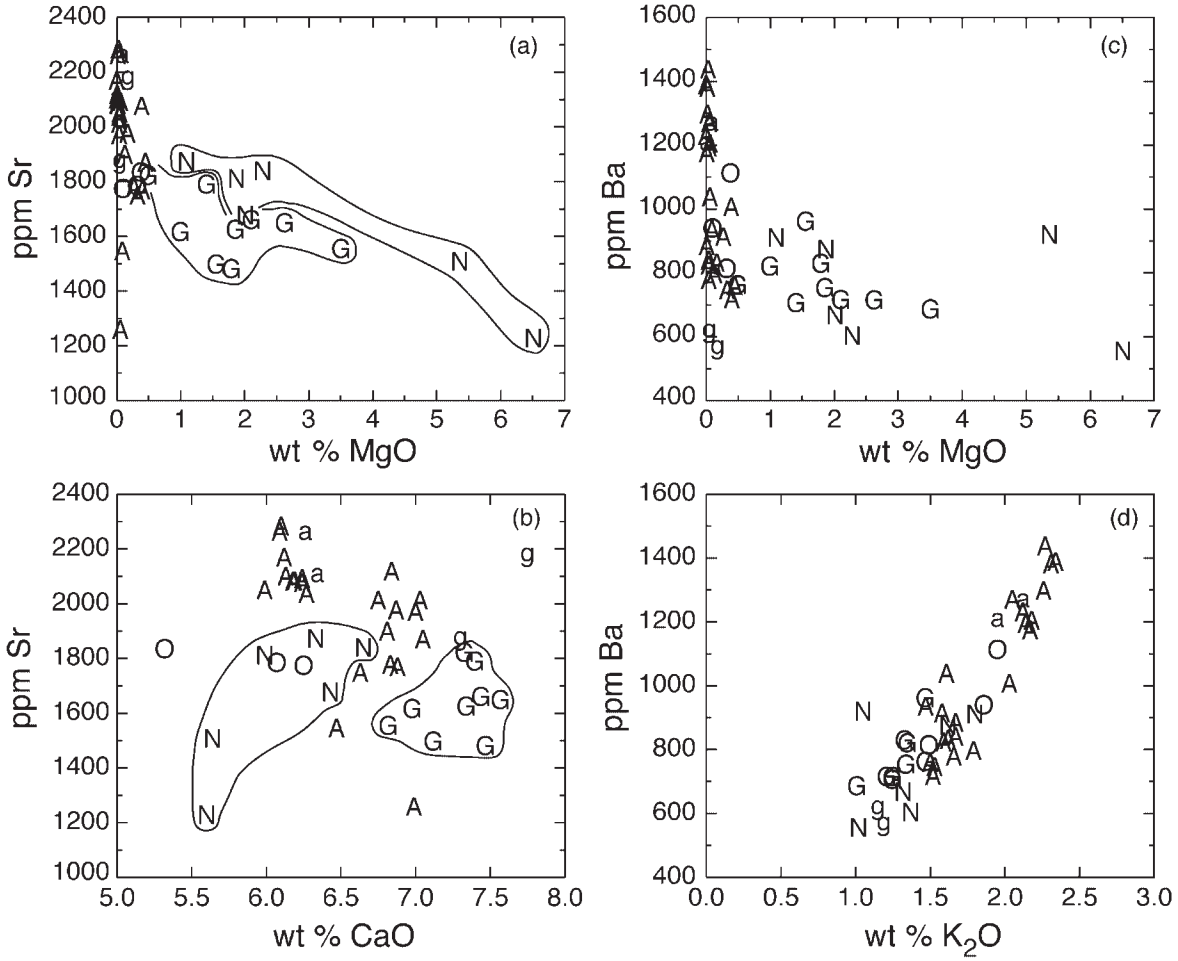

Fig. 9. Variation diagrams for selected trace elements in rocks of the Labrieville massif (symbols as in Fig. 2). (a) Sr vs MgO; (b) Sr vs CaO; (c) Ba vs MgO; (d) Ba vs K_2O.

amounts of Sr increase in the same sequence. Therefore, the alkalic compositions at Labrieville can be explained most easily by crystallization from an alkalic parental magma, which probably differed considerably from the broadly tholeiitic magmas that gave rise to the Skaergaard and Kiglapait layered intrusions. It has been argued by some investigators (e.g. Gray, 1987) that alkalic compositions in massif anorthosites result from crustal contamination of mantle-derived basalt containing otherwise normal levels of K and Na. At Labrieville, however, the combined Rb–Sr, Sm–Nd, and U–Th–Pb isotopic data contraindicate such contamination (Owens *et al.*, 1994). Our preferred interpretation for the alkalic nature of this massif is that it reflects the composition of the source region, which could be alkali-enriched lithospheric mantle (see Owens, 1998) or lower crust (see Duchesne *et al.*, 1999; Schiellerup *et al.*, 2000).

The Sr and Ba concentrations in Labrieville rocks are compared with those from St. Urbain and Morin anorthosites in Fig. 14. Concentrations of both elements show a crude systematic increase in the sequence Morin → St. Urbain → Labrieville, and correlate with the trend of decreasing normative An (or increasing normative Or) illustrated in Fig. 13. Also shown for comparison in Fig. 14 are data for anorthosites from the Nain complex, Labrador (Xue & Morse, 1993), which are also distinct from Labrieville.

The extreme levels of these trace elements in the Labrieville massif make it the most Sr- and Ba-rich anorthosite yet reported. Not only is Labrieville distinctive in this respect, but it appears that these feldspar compositions are extreme relative to those reported from virtually all igneous rock types. To illustrate this feature, the Sr and Ba concentrations in anorthosite (rocks with >95% normative feldspar) and plagioclase megacrysts from Labrieville are compared with data on plagioclase compiled by Blundy & Wood (1991) in their studies of Sr and Ba partitioning (Fig. 15). Most samples from

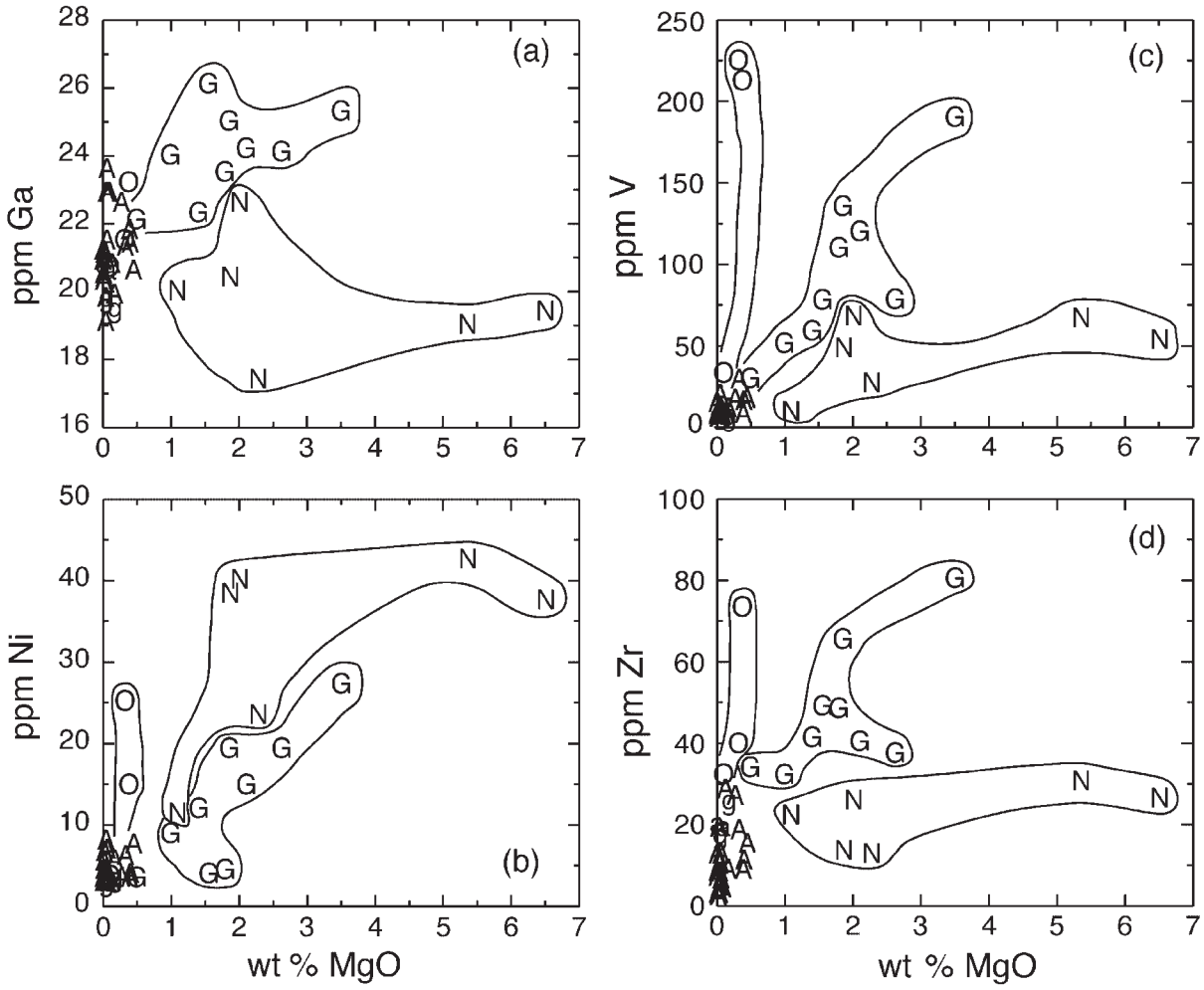

Fig. 10. MgO-variation diagrams for selected trace elements in rocks of the Labrieville massif (symbols as in Fig. 2): (a) Ga; (b) Ni; (c) V; (d) Zr.

Labrieville have Sr and Ba concentrations higher than those reported in other studies, but are most like compositions reported by Berlin & Henderson (1969) for trachyte or phonolite, or by Liotard *et al.* (1979) for andesite or rhyolite.

These high levels of Sr and Ba can be accounted for in (at least) two ways: crystallization from liquids with extremely high Sr and Ba assuming 'typical' plagioclase–melt partition coefficients, or crystallization of plagioclase having unusually high partition coefficients for these elements. With respect to the latter interpretation, Blundy & Wood (1991) reasoned on thermodynamic grounds that D_{Sr} (plag/liq) and D_{Ba} (plag/liq) should both increase with decreasing An content. Thus, much higher partition coefficients might apply in the case of the low-An Labrieville plagioclase. Application of the semi-empirical relationships between D and X_{An} derived by Blundy & Wood (1991) yields $D_{Sr} = 4{\cdot}6$ and $D_{Ba} = 0{\cdot}9$ for plagioclase having An/Ab like Labrieville (using $T = 1200°C$). Use of these calculated partition coefficients implies crystallization from less-extreme liquid compositions ($\sim$400 ppm Sr and 1100 ppm Ba), although Ba is still relatively high.

On the other hand, Morse (1992) rejected the Blundy & Wood crystal-chemical model for Sr partitioning in plagioclase, and argued instead for a strong control by liquid composition. Values of D_{Sr} (plag/liq) derived by Morse (1982*a*) from data in the Kiglapait intrusion vary from $\sim 1{\cdot}5$ to 2 over the course of crystallization. Using a typical Kiglapait value of 1·8, calculated liquid compositions in equilibrium with Labrieville plagioclase ($\sim$2000 ppm Sr) would contain $\sim$1100 ppm Sr, nearly three times the value determined from the Blundy & Wood model.

The effect of pressure on D_{Sr} (plag/liq) has recently been evaluated experimentally by Vander Auwera *et*

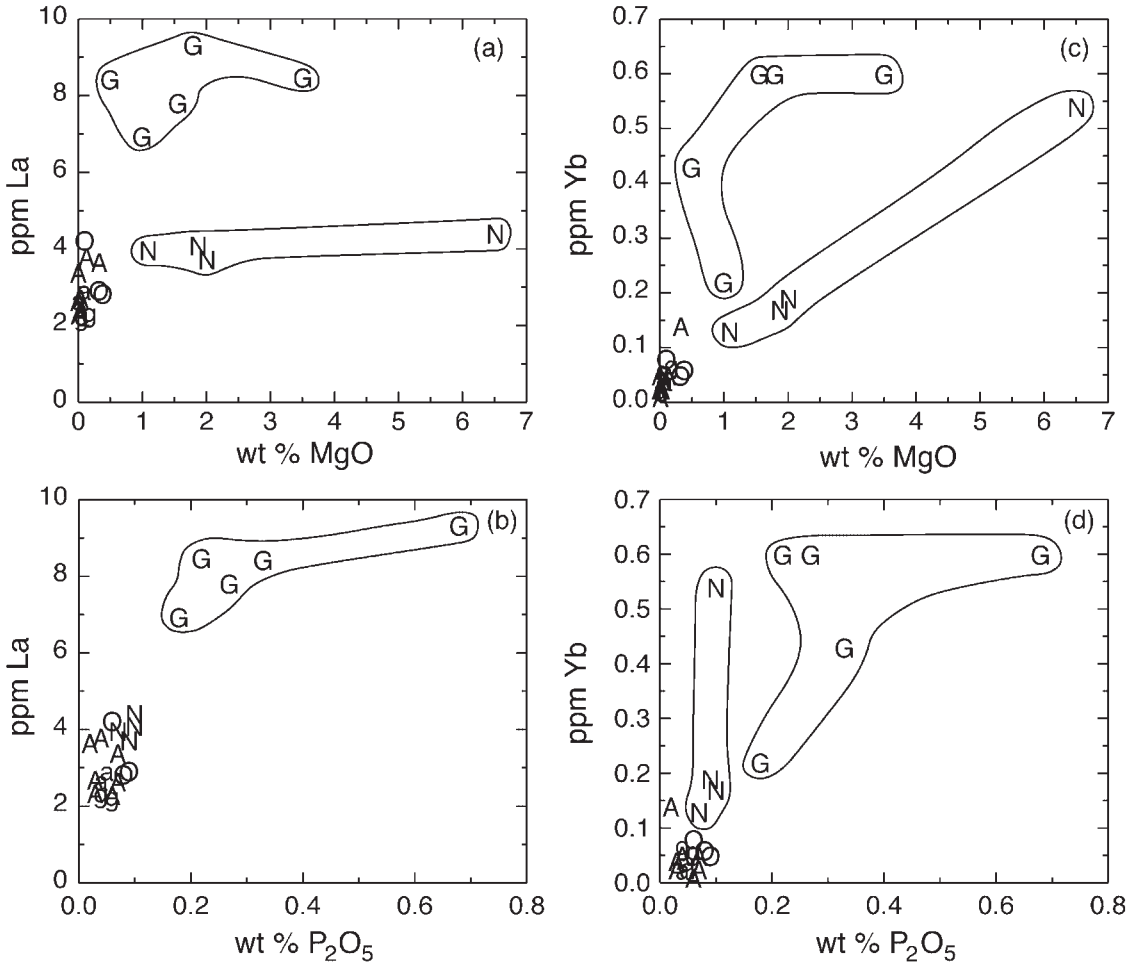

Fig. 11. Variation diagrams for selected REE in rocks of the Labrieville massif (symbols as in Fig. 2): (a) La vs MgO; (b) La vs P_2O_5; (c) Yb vs MgO; (d) Yb vs P_2O_5.

al. (2000), who concluded that the partition coefficient decreases slightly with increasing pressure. Thus, the elevated levels of Sr in Labrieville plagioclase probably cannot be attributed to higher pressures of crystallization than for other anorthosites. Vander Auwera *et al.* (2000) also showed that the relationship between D_{Sr} (plag/liq) and X_{An} derived by Blundy & Wood (1991) consistently overestimated D_{Sr} relative to the values determined from their experiments, and that the disparity increased with increasing pressure by as much as a factor of three. In contrast, values of D_{Sr} based on the Morse (1982*a*) model slightly underestimated the measured values. Nevertheless, Vander Auwera *et al.* (2000) concluded from all of their experiments that a D_{Sr} (plag/liq) value of 1·8 is probably appropriate for anorthositic magmas crystallizing at a pressure of 10 kbar. A reasonable inference from all of this work is that atypically high values of D_{Sr} (plag/liq) are probably not applicable at Labrieville. On the other hand, the elevated levels of Ba in the anorthositic feldspars are entirely consistent with their highly potassic nature, such that D_{Ba} (plag/liq) may have been ≥ 1 (see below). Therefore, we prefer an interpretation involving high-Sr and high-Ba liquids as the most plausible explanation for Labrieville feldspar compositions.

The nature and implications of chemical variations among Labrieville rocks

The major- and trace-element variation diagrams presented in Figs 7–11 clearly demonstrate the importance of mineral–mineral mixing in controlling the whole-rock compositions of the various Labrieville samples. This result is perhaps not surprising, but it has profound implications for the 'chemical assembly' (Dymek, 1989) of the rocks at Labrieville, as well as for the interpretation of variation diagrams for anorthositic rocks in general. Specifically, do whole-rock samples represent cumulus

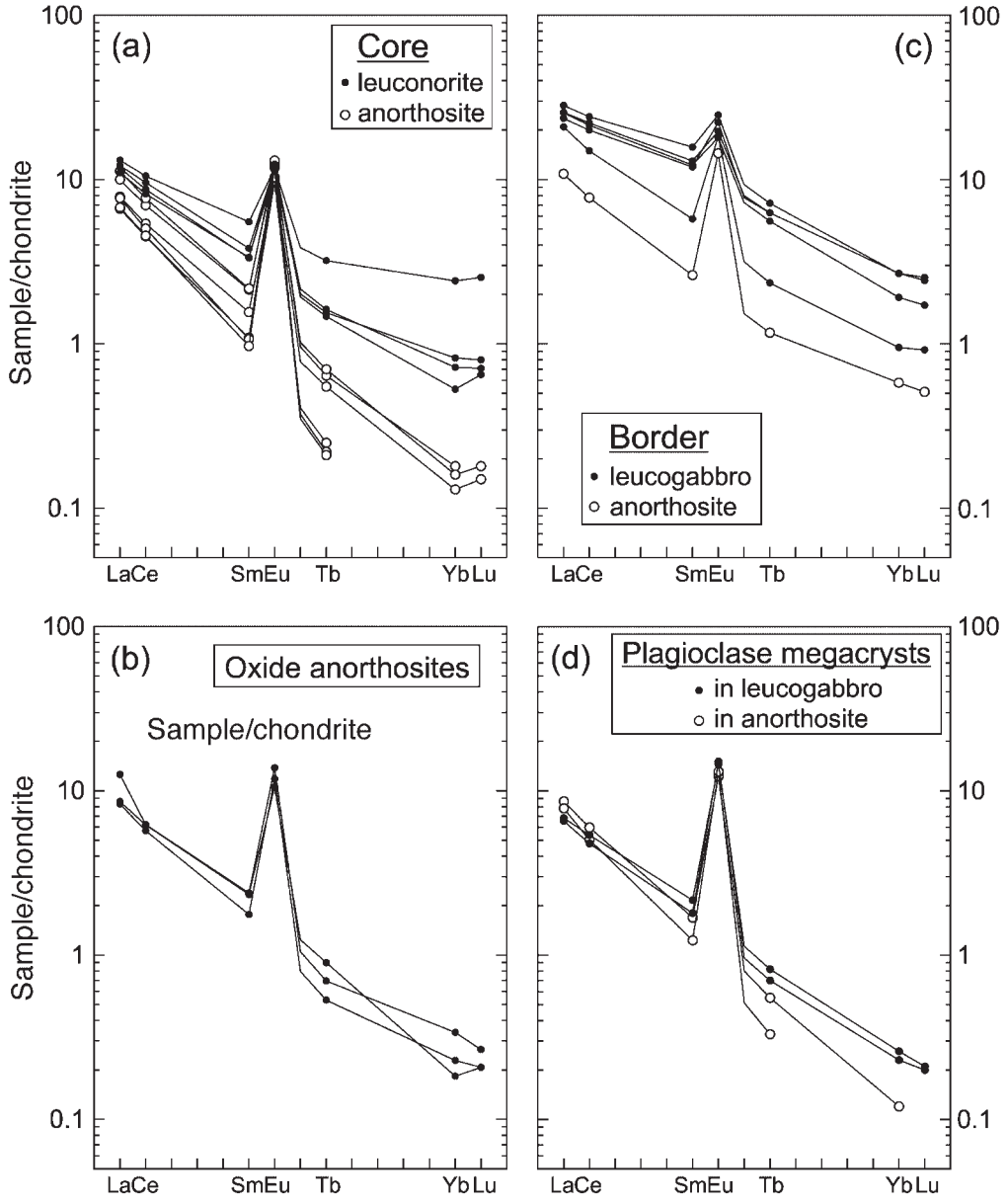

Fig. 12. Chondrite-normalized concentrations of REE in various Labrieville rock types. Data points for Yb and Lu are not plotted for those samples in which only a maximum value could be determined. The chondrite values used in this plot are taken from Anders & Ebihara (1982) multiplied by 1·38, which represents a least-squares best fit to the earlier chondrite composite of Haskin *et al.* (1968) (R. Korotev, personal communication, 1987).

plagioclase plus mafic minerals that crystallized from trapped liquid? Or do the rocks consist primarily of variable mixtures of cumulus minerals, with negligible trapped-liquid component? In this regard, Simmons & Hanson (1978) and Ashwal & Seifert (1980) assumed, largely on the basis of REE contents, that anorthositic rocks from the Adirondacks (and Nain) could be modeled as mixtures of cumulus plagioclase plus trapped (possibly parental) liquid. These investigators inferred furthermore that the mafic fractions of rocks (e.g. in leucogabbro) represent the *in situ* crystallization products of this trapped-liquid component. The Labrieville data provide a means of testing this hypothesis.

As reasoned by Salpas *et al.* (1983), anorthositic rocks consisting primarily of cumulus plagioclase plus variable amounts of trapped liquid (of essentially fixed composition) should yield a data array with a positive slope in diagrams such as Figs 8f (P_2O_5 vs MgO) and 11a

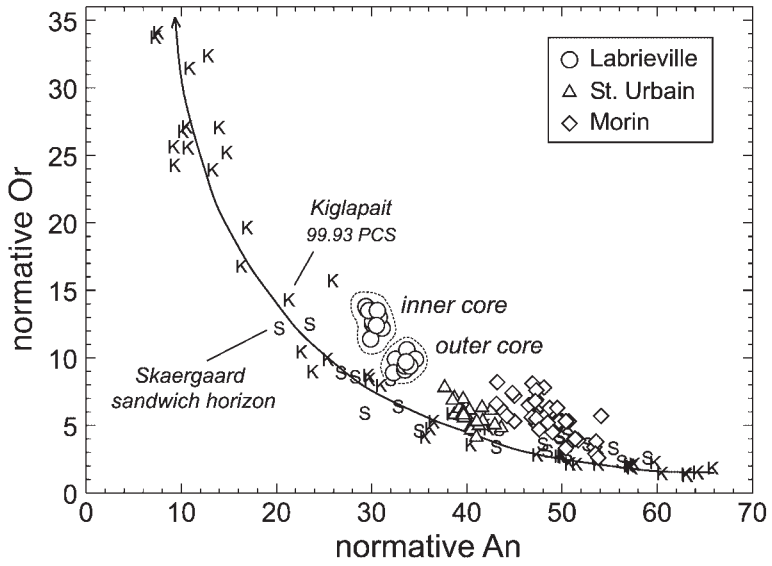

Fig. 13. Plots of whole-rock normative An vs Or for anorthositic rocks (>95% normative feldspar) of the Labrieville massif (this study) compared with data for the St. Urbain and Morin massifs (R. F. Dymek, unpublished results, 1999). Also shown are whole-rock compositions and a generalized trend arrow for the Kiglapait Intrusion, Labrador (data from Morse, 1981) and the Skaergaard Intrusion, Greenland (data from McBirney, 1989). (Note the displacement of the massif anorthosite data from the trend of the basaltic intrusions, and note also the difference between the Kiglapait and Skaergaard data.) For Kiglapait, the most evolved compositions are from upper-zone ferrosyenites and ferromonzonites that crystallized very late. For reference, a sample from the 99·93% solidified (PCS) level is marked. The two most evolved samples in the Skaergaard Intrusion are from the Sandwich Horizon.

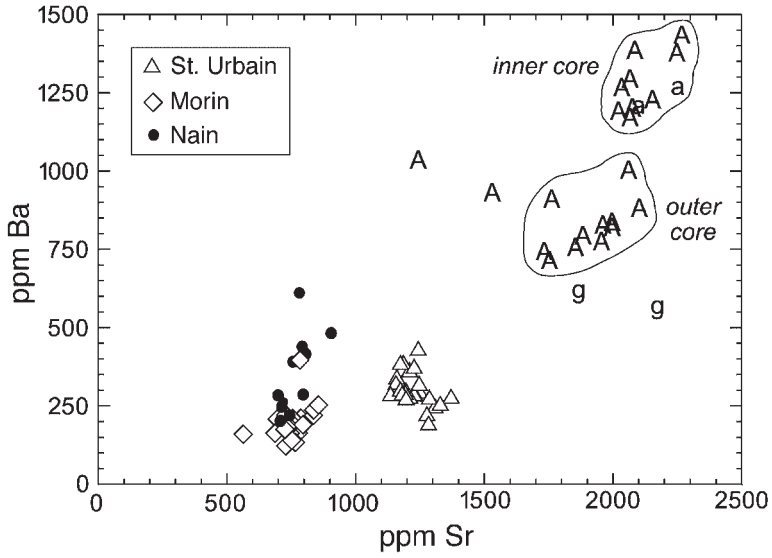

Fig. 14. Sr vs Ba in anorthositic rocks of the Labrieville massif (this study) compared with data for the St. Urbain and Morin massifs (R. F. Dymek, unpublished results, 1999). Also shown for comparison are data from the Nain anorthosite complex, Labrador (Xue & Morse, 1993). [Note that anorthosites from the inner and outer core zones fall into separate fields (see text for discussion).] The two anorthosite samples with lower Sr occur near the hemoilmenite ore deposit.

(La vs MgO), reflecting plagioclase–liquid mixing. Such trends result from the fact that both elements on each plot are incompatible in plagioclase and, therefore, the levels of both should increase with the amount of trapped liquid in the rock. P_2O_5 and La are also incompatible in pyroxene, whereas MgO is compatible. Therefore, rocks consisting primarily of variable quantities of cumulus plagioclase + cumulus pyroxene (+Fe–Ti oxide) should yield a broadly horizontal data array, reflecting plagioclase–pyroxene mixing. It can be seen in Figs 8f and 11a

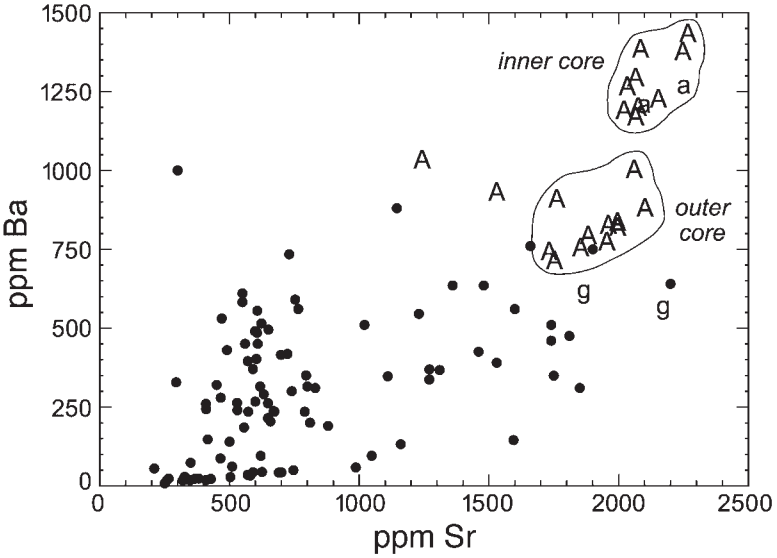

Fig. 15. Sr vs Ba in anorthositic rocks of the Labrieville massif compared with the dataset on plagioclase compiled by Blundy & Wood (1991) in their study of plagioclase–melt trace-element partitioning.

that the data for core anorthosites, oxide-anorthosites, and leuconorites yield essentially horizontal trends, consistent with the interpretation that these rocks represent variable mixtures of cumulus plagioclase, orthopyroxene, and hemoilmenite, with negligible trapped-liquid component. Likewise, the good correlation between Yb and MgO shown by the leuconorites (Fig. 11c) indicates that these rocks represent primarily plagioclase–orthopyroxene mixtures.

The amount of trapped liquid component in relatively pure core anorthosite can be evaluated by comparing the compositions of plagioclase megacrysts and their associated anorthosite host rocks. In the two measured cases, the compositions of megacrysts are essentially the same as their hosts (Table 6), even for P_2O_5 and the REE (in one case the megacryst actually contains higher P_2O_5 and REE than its host). Thus, these samples of anorthosite appear to be devoid of any trapped liquid component (which would presumably contain a higher concentration of these elements than the cumulus plagioclase).

The horizontal data arrays for P_2O_5 (Fig. 8f) and La vs MgO (Fig. 11a) clearly demonstrate that there is no correlation between potential trapped liquid components and the amount of mafic material in the leuconorites. However, it is an oversimplification to view the leuconorites as pure orthopyroxene–plagioclase ($\pm$ ilmenite) cumulates because they tend to contain higher amounts of the LREE than anorthosites (Fig. 12a). Rocks that are simple orthopyroxene–plagioclase mixtures should show somewhat LREE-depleted patterns relative to anorthosite, because partition coefficients for LREE in orthopyroxene are less than those in plagioclase (e.g. Dunn & Sen, 1994). The enhanced LREE in the leuconorites relative to anorthosites may be a trapped liquid effect, which would be consistent with slightly higher P_2O_5 in leuconorites (Fig. 11b).

In contrast to the core lithologies, the data for border leucogabbros plot away from anorthosite in a direction of increasing MgO, P_2O_5, La, and Yb (Figs 8f and 11a and c), but the distribution of data points is somewhat scattered and clearly does not define a simple trend. If these rocks represent mixtures of cumulus plagioclase plus variable amounts of trapped liquid, then the composition of the trapped-liquid component must have been different in each case. Alternatively, the leucogabbros might simply represent variable mixtures of cumulus plagioclase + pyroxene + Fe–Ti oxide + apatite, once apatite became a cumulus mineral, but the scatter in the data implies that these minerals do not occur in simple, cotectic proportions. Some mechanical sorting of minerals, especially apatite, is implied. A trapped-liquid component might be present in addition to several cumulus minerals, but in this case it would be more difficult to recognize. We consider the latter interpretation (i.e. the presence of cumulus apatite) to be the one that is most consistent with the chemical data, and with the petrographic observation of coarse apatite grains in many thin sections of leucogabbro. In either case, the REE patterns of the leucogabbros show that they were assembled in a different fashion than the core leuconorites (Fig. 12).

A larger dataset (including REE analyses of individual minerals) would be desirable to evaluate more fully the cause of chemical variation in the Labrieville rocks. However, the above analysis is sufficient to demonstrate that most rocks, even the more mafic varieties, consist

primarily of variable mixtures of cumulus minerals, rather than mixtures of plagioclase + trapped liquid (see Simmons & Hanson, 1978; Ashwal & Seifert, 1980). This result implies the efficient expulsion of trapped liquid from all rock types in the massif, not just from relatively pure anorthosite. We infer that the expulsion of liquid occurred during magmatic crystallization or recrystallization accompanying diapiric rise of the anorthosite mass that produced its dome shape (see Dymek, 1999).

The fact that most rocks at Labrieville are made up of variable proportions of cumulus minerals has important implications for the interpretation of whole-rock variation diagrams as applied to anorthositic rocks in general. Regardless of the index of differentiation used (SiO_2, MgO, or some combination of oxides), any variation diagram applied to these rocks will normally reflect the effects of mineral–mineral mixing (e.g. plagioclase + orthopyroxene), rather than the liquid line of descent of a magma. Therefore, any suggestion that such variation diagrams illustrate the differentiation trend of anorthosite parental magmas should be viewed with skepticism. For example, Buddington (1972), Ashwal (1978, 1993), and McLelland & Whitney (1990), among others, have argued that rocks of the anorthosite and mangerite (or charnockite) suites in the Adirondacks (and elsewhere) show different and opposing differentiation trends on variation diagrams, and thus originated from separate parental magmas. This assertion has been taken as evidence for 'bimodal magmatism' in the evolution of anorthosite complexes. However, if the results from Labrieville have more general application, then this approach has serious limitations. Specifically, the strong effects of accumulation and mineral–mineral mixing are likely to dominate the distribution of data for anorthositic rocks, making the recognition of a true liquid differentiation trend difficult. Therefore, we suggest that variation diagrams, although useful for illustrating whole-rock data, are not the best means of evaluating anorthositic differentiation trends, or possible genetic relationships between anorthosite and the felsic rocks of the mangerite suite.

Differentiation of the Labrieville massif

An unanticipated outcome of our whole-rock compositional dataset was the recognition of an 'inner core' consisting of rocks with average normative compositions $\sim An_{30}Or_{13}$ and an 'outer core' averaging $\sim An_{35}Or_{10}$ (see Fig. 13); in addition, Ba and Sr are higher in anorthosites of the inner core than the outer core (see Fig. 14). We note that normative An contents in border zone rocks overlap entirely with those of the outer core, and that plagioclase megacrysts in the border are more calcic than those in the core (Fig. 2). The existence of these zones with different compositions implies some sort of differentiation during crystallization of the anorthositic portion of the Labrieville massif. If feldspar composition is used as the sole monitor of differentiation, the massif appears to have crystallized inward (or from the top down before doming) because inner core rocks are richer in Na and K (and Ba) than those in the outer core and border.

However, an interpretation of inward differentiation is problematic for several reasons. First, pyroxene X_{Mg} decreases from the inner core through the outer core to the border (Fig. 6) implying differentiation outward towards the rim (see Anderson, 1966). Second, inward differentiation is at odds with the higher Sr in inner core rocks, unless plagioclase fractionation was accompanied by vast amounts of mafic material. Such mafic material is certainly not present in the field, and there is no evidence to support arguments for missing, buried mafic cumulates (Owens & Dymek, 1995). Third, the change in mineral assemblage at the pluton scale from core to border is more consistent with outward differentiation. Specifically, the border rocks contain more phases than core rocks, including two pyroxenes, two Fe–Ti oxides, and apatite. The addition of phases to a crystallizing assemblage, rather than their elimination, is much more in keeping with all observational, experimental, and theoretical investigations of crystallizing magmas.

For the above reasons, we consider inward differentiation of the massif to be highly unlikely and favor instead the alternative scenario of outward differentiation from inner core to outer core to border (or from the bottom upward before doming). However, this interpretation is not without difficulty, as it requires explanation of (at least) two additional features. First, Ba concentrations decrease in this proposed fractionation sequence. This finding implies that D_{Ba} (plag/liq) >1, which we believe is a plausible crystal-chemical effect related to high K in Labrieville plagioclase; the fact that Ba correlates well with K (Fig. 6d) supports this interpretation. Second, but more difficult to explain, is that outward differentiation requires plagioclase compositions to become more calcic (and less potassic) from inner core through outer core to border. Such a trend is, of course, opposite to that of plagioclase compositional variation expected during cooling.

One possible explanation for this postulated reverse fractionation trend is that the Labrieville magma was progressively contaminated with a high-Ca, low-K component during crystallization. A convenient contaminant of this type would be marble, but no marble occurs in the vicinity of this massif. Another possible contaminant is labradorite anorthosite, such as represented by the nearby Lac St. Jean massif (Fig. 1). In fact, a few xenoliths of labradorite anorthosite do occur in the Labrieville pluton (see Anderson, 1966; Dymek & Owens, 1998*a*).

Contamination by calcic plagioclase would have essentially no effect on Fe/Mg in mafic phases, thus accounting for the 'normal' cryptic variation recorded by pyroxene, but potentially could alter the An content of crystallizing plagioclase in a profound way. On the basis of theoretical analyses of Bowen (1928), McBirney (1979), and Morse (1980), assimilation of plagioclase that is more calcic than that in equilibrium with a magma occurs by crystallization of additional equilibrium-composition plagioclase, whereas the xenocrystic plagioclase is made over through diffusive reaction into a composition in equilibrium with the melt. As a result, such assimilation is a 'self-defeating' process because it consumes melt (Morse, 1980). The net effect of such a process in the case of perfect equilibrium would be to raise the temperature slightly (because the assimilative reaction in this case is slightly exothermic) and promote crystallization of a more calcic plagioclase (Bowen, 1928). Under natural conditions, experiments of Tsuchiyama (1985) suggest that the effects are probably less striking and most labradorite xenoliths would be relatively inert in a Labrieville magma (assuming that the xenoliths were actually incorporated into a liquid rather than a highly crystalline mush). The fact that at least some of the xenoliths can be still recognized as compositionally and physically distinct entities demonstrates that re-equilibration with the melt did not go to completion. Thus, from a consideration of thermal and mass-balance constraints, assimilation seems an ineffective means of producing a reversal of plagioclase compositional evolution at the pluton scale.

Yet another explanation that warrants consideration involves the effects of H_2O on plagioclase compositional relationships. Specifically, it has been demonstrated experimentally, first by Yoder (1969) and more recently by Sisson & Grove (1993), that an increase in the amount of water in mafic magmas results in the crystallization of a more calcic plagioclase than in dry magmas. Indeed, Sisson & Grove (1993) documented clear increases in $(Ca/Na)_{plag}/(Ca/Na)_{liquid}$ with increases in the amount of water in their experiments. Thus, it is conceivable that a build-up of H_2O during crystallization of the oxidized and water-bearing Labrieville magma resulted in the production of progressively more calcic plagioclase as differentiation proceeded. That the Labrieville magma was fluid bearing (but certainly not vapor saturated) is suggested by the ubiquitous presence of biotite throughout the massif, patches of calcic myrmekite (see Dymek & Schiffries, 1987), and the oxidized nature of the hemoilmenite. In addition, the typically altered character of border leucogabbros could be a deuteric effect, related to this proposed increase in water content.

A final possibility is that the inner and outer core zones crystallized under slightly different conditions, perhaps at different levels in the crust, irrespective of whether the parental magma was water bearing. In this scenario, the inner core zone would commence crystallization at 'high' pressure. After sufficient plagioclase accumulation was achieved, the inner core began to rise as a magmatic diapir carrying with it an envelope of residual, more mafic liquid. If our estimate of the size of the inner core in map view is approximately correct (and the units are equidimensional vertically), this zone probably makes up no more than 50% of the massif (Fig. 3). Thus, if the inner core represents a zone of initial crystal accumulation, the proportion of crystals to liquid before doming would appear to lie well below the limit of ~65% for movement of plagioclase-rich crystal mushes (Longhi *et al.*, 1993). At a higher crustal level (i.e. slightly lower pressure), the outer core and border zones crystallized. The lack of foliation in parts of the border zone suggests that it crystallized close to the level of final emplacement, i.e. after upward diapiric movement had ceased. We note that jotunites, rocks that we consider to be residual to crystallization of the massif (Owens *et al.*, 1993), also occur in association with border leucogabbros.

Polybaric crystallization is supported by experimental studies, and would be consistent with certain parts of currently popular models for anorthosite petrogenesis. For example, Green (1969) showed that the liquidus plagioclase in several melt compositions (including anorthositic) becomes more sodic and potassic with increasing pressure. More recently, Longhi *et al.* (1993) documented similar shifts in plagioclase composition with pressure, and observed that the shift is ~1% An/kbar (although this value varies somewhat with bulk composition). Thus, the change from a higher-Ab and -Or plagioclase (inner core) to a lower-Ab and -Or plagioclase (outer core) at Labrieville, which involves only a slight difference in composition (Fig. 13), would require a pressure drop of <5 kbar if these experimental results are applied.

Longhi *et al.* (1993) extended this observation about the pressure effect on plagioclase composition to a more elaborate model involving polybaric fractionation for massif anorthosites. Longhi *et al.* (1993) puzzled over the apparent lack of reverse zoning at the grain scale in anorthosites and suggested that this was due to plagioclase–melt re-equilibration under very slow cooling conditions (coupled with the fact that plagioclase-rich crystal mushes should show only a small shift in An content with decreasing pressure). Nonetheless, pluton-scale reversals in plagioclase composition are entirely compatible with the experimental evidence, provided that early-formed, high-pressure portions of a pluton are effectively isolated from the liquid at lower pressure.

As a final observation, the presence of compositionally distinct zones is a feature that is apparently not unique to Labrieville. Our recent work on the nearby Mattawa massif (Owens & Dymek, 1998, 1999*b*) has shown a similar zonal arrangement, and the anorthosites at St.

Urbain, Lac à Jack, and Château-Richer appear to have more calcic plagioclase near their borders (R. F. Dymek, unpublished results, 1999). Hence, pluton-scale reverse zoning might be a characteristic feature of these andesine anorthosites, indicating that they evolved in a similar fashion, regardless of the mechanism.

CONCLUDING REMARKS

The results presented above indicate that the Labrieville massif is a concentrically zoned pluton that differs significantly in composition from other massif anorthosites. Differentiation involved first the crystallization (and accumulation) of plagioclase, followed by hemoilmenite (which locally accumulated into a sizable ore body), then orthopyroxene (locally as plagioclase-lamellae-bearing megacrysts; see Owens & Dymek, 1995), then clinopyroxene, then magnetite, and finally apatite. The corresponding rock types range outward from an anorthosite inner core, through a leuconorite–anorthosite outer core, to a leucogabbro–anorthosite rim. Pyroxene and plagioclase compositions (as revealed by X_{Mg}, normative percent An–Or, ppm Ba and Sr) change more or less systematically across the pluton but seem to indicate different directions for core-to-rim differentiation. We favor outward (or upward before doming) differentiation under the influence of decreasing pressure, which was possibly accompanied by increasing H_2O content in the silicate liquid.

The Labrieville rocks (anorthosite–leuconorite–leucogabbro) are interpreted to be cumulates largely devoid of trapped liquid. As such, most trends on variations diagrams are those of accumulation, plagioclase dilution, and mineral mixing, and any attempt to use bulk compositions of anorthositic rocks to reproduce liquid lines of descent is fraught with uncertainty.

Because of their cumulate character, the Labrieville rocks themselves provide little direct evidence for the nature of their parental magma. Nevertheless, we can draw some general and important indirect inferences about that parental magma as follows: (1) it must have been alkalic to produce the extremely Na- and K-rich plagioclase of the massif; (2) similarly, it contained extreme concentrations of Ba and Sr, or concentrations of those elements high enough to yield plagioclase having Ba and Sr higher than virtually any other known feldspar; (3) the magma must have been highly oxidizing, as revealed by the ubiquitous presence of hemoilmenite, while yielding relatively Mg-rich orthopyroxene. Two additional features (Ti/V and Ga/Al ratios) noted here and discussed in detail by us previously (Owens *et al.*, 1993) are very high compared with other rock types. Collectively, the mineralogical and chemical features of Labrieville indicate that this parental magma was unlike the tholeiitic magmas that gave rise to layered intrusions such as the Skaergaard or Kiglapait.

We note that troctolitic or gabbroic rocks are rare to absent from any of the andesine anorthosites of this region. Thus, we find no evidence for the troctolitic or high-Al gabbroic magmas that have been suggested as parental to massif anorthosites elsewhere (e.g. Fram & Longhi, 1992; Mitchell *et al.*, 1996; Markl & Frost, 1999; Scoates & Mitchell, 2000). On the other hand, jotunite dikes in this region probably approach the composition of liquids, but they contain feldspars and pyroxenes that are too evolved for them to be viable as parental magmas for associated anorthosites (Owens *et al.*, 1993). Nevertheless, we find arguments for parental magmas of broadly jotunitic character appealing (seeVander Auwera & Longhi, 1994; Vander Auwera *et al.*, 1998, 2000).

Despite its unusual composition, the radiogenic isotope data for Labrieville indicate derivation from the mantle or juvenile sources in the deep crust at ~1·01 Ga, subsequent to the culmination of the Grenville orogeny (Owens *et al.*, 1994). We emphasize that Labrieville is one of several hemoilmenite-bearing, late- to post-orogenic, andesine anorthosites found in a belt cutting across this region of the Grenville Province (Fig. 1; Dymek & Owens, 1998*b*). We consider it likely that the mineralogical and chemical characteristics of these anorthosites are somehow related to their post-tectonic emplacement (Owens *et al.*, 1994). Thus, their origin may be linked in some way with the Grenville orogeny, and earlier models for massif anorthosites involving aborted continental rifting under anorogenic conditions do not apply in this case (e.g. Emslie, 1978; Morse, 1982*b*; Windley, 1989; McLelland & Whitney, 1990). In contrast, crustal thickening induced by the final (Ottowan) phase of the Grenville orogeny promoted thermal conditions that resulted in the formation of a distinctive type of magma that might be unique to deep processes in continent–continent collisional orogens.

ACKNOWLEDGEMENTS

B.E.O. thanks M. S. Smith, J. P. Icenhower, and M. W. Rockow for field assistance, and A.T. Anderson, Jr, for helpful discussions during the early phases of this investigation. We also thank R. A. Couture, D. K. Kremser, and R. L. Korotev for maintenance of the X-ray fluorescence, electron microprobe, and neutron activation facilities, respectively, at Washington University. Much of the work reported here was supported by NSF Grants EAR88-16977 and EAR90-19366 to R.F.D., and by additional grants from the Geological Society of America and Sigma Xi. We thank R. F. Emslie, M. D. Higgins, and J. N. Mitchell for their thoughtful reviews.

REFERENCES

Albee, A. L. & Ray, L. (1970). Correction factors for electron probe microanalysis of silicates, oxides, carbonates, phosphates and sulfates. *Analytical Chemistry* **42**, 1408–1414.

Anders, A. E. & Ebihara, M. (1982). Solar-system abundances of the elements. *Geochimica et Cosmochimica Acta* **46**, 2363–2380.

Anderson, A. T., Jr (1962). Preliminary report on Catherine Lake area, Chicoutimi County. *Quebec Department of Natural Resources Preliminary Report* **488**, 7 pp.

Anderson, A. T., Jr (1963). A contribution to the mineralogy and petrology of the Brulé Lake anorthosite massif, Quebec. Ph.D. thesis, Princeton University, Princeton, NJ.

Anderson, A. T., Jr (1966). Mineralogy of the Labrieville anorthosite, Quebec. *American Mineralogist* **51**, 1671–1711.

Anderson, A. T., Jr (1969). Massif-type anorthosite: a widespread Precambrian igneous rock. In: Isachsen, Y. W. (ed.) *Origin of Anorthosite and Related Rocks. New York State Museum and Science Service Memoir* **18**, 47–55.

Anderson, A. T., Jr & Morin, M. (1969). Two types of massif anorthosites and their implications regarding the thermal history of the crust. In: Isachsen, Y. W. (ed.) *Origin of Anorthosite and Related Rocks. New York State Museum and Science Service Memoir* **18**, 57–69.

Ashwal, L. D. (1978). Petrogenesis of massif-type anorthosites: crystallization history and liquid line of descent of the Adirondack and Morin Complexes. Ph.D. thesis, Princeton University, Princeton, NJ.

Ashwal, L. D. (1993). *Anorthosites*. Berlin: Springer, 422 pp.

Ashwal, L. D. & Seifert, K. E. (1980). Rare-earth-element geochemistry of anorthosite and related rocks from the Adirondacks, New York, and other massif-type complexes. *Geological Society of America Bulletin, Part II* **91**, 659–684.

Ashwal, L. D. & Twist, D. (1994). The Kunene complex, Angola/Namibia: a composite massif-type anorthosite complex. *Geological Magazine* **131**, 579–591.

Bence, A. E. & Albee, A. L. (1968). Empirical correction factors for the electron microanalysis of silicates and oxides. *Journal of Geology* **76**, 382–403.

Berlin, R. & Henderson, C. M. B. (1969). The distribution of Sr and Ba between the alkali feldspar, plagioclase and groundmass phases of porphyritic trachytes and phonolites. *Geochimica et Cosmochimica Acta* **23**, 247–255.

Blundy, J. D. & Wood, B. J. (1991). Crystal-chemical controls on the partitioning of Sr and Ba between plagioclase feldspar, silicate melts, and hydrothermal solutions. *Geochimica et Cosmochimica Acta* **55**, 193–209.

Bowen, N. L. (1917). The problem of the anorthosites. *Journal of Geology* **25**, 209–243.

Bowen, N. L. (1928). *The Evolution of the Igneous Rocks*. New York: Dover, 332 pp.

Buddington, A. F. (1972). Differentiation trends and parental magmas for anorthositic and quartz mangeritic series, Adirondacks, New York. In: Shagam, R., Hargraves, R. B., Morgan, W., VanHouten, F., Burk, C., Holland, H. & Hollister, L. (eds) *Studies in Earth and Space Science. Geological Society of America, Memoir* **132**, 477–488.

Couture, R. A. & Dymek, R. F. (1996). A reexamination of absorption and enhancement effects in X-ray fluorescence trace element analysis. *American Mineralogist* **81**, 639–650.

Couture, R. A., Smith, M. S. & Dymek, R. F. (1993). X-ray fluorescence analysis of silicate rocks using fused glass discs and a side-window Rh source tube: accuracy, precision and reproducibility. *Chemical Geology* **110**, 315–328.

Duchesne, J. C., Liégeois, J. P., Vander Auwera, J. & Longhi, J. (1999). The crustal tongue melting model and the origin of massive anorthosites. *Terra Nova* **11**, 100–105.

Dunn, T. & Sen, C. (1994). Mineral/matrix partition coefficients for orthopyroxene, plagioclase, and olivine in basaltic to andesitic systems: a combined analytical and experimental study. *Geochimica et Cosmochimica Acta* **58**, 717–733.

Dymek, R. F. (1981). Reverse zoning in plagioclase from labradorite anorthosite, St. Urbain massif, Quebec: retrograde plag–pyx reaction? *Geological Society of America, Abstracts with Program* **13**, 444.

Dymek, R. F. (1989). Chemical assembly of anorthositic rocks at St-Urbain, Quebec. *Geological Association of Canada/Mineralogical Association of Canada, Program with Abstracts* **14**, 51–52.

Dymek, R. F. (1990). Petrogenetic implications of Ga/Al ratios in massif anorthosites. *Geological Society of America, Abstracts with Program* **22**, 300.

Dymek, R. F. (1999). Diapirism in aid of anorthosite purification. *EOS Transactions, American Geophysical Union* **80**, 366.

Dymek, R. F. & Owens, B. E. (1996). Petrogenetic relationships among FTP-rocks of the anorthosite suite (nelsonites, jotunites, OAGNs, and oxide ores) as revealed by REE characteristics of separated apatites. *Geological Society of America, Abstracts with Program* **28**, 288.

Dymek, R. F. & Owens, B. E. (1998*a*). Labradorite anorthosites found within (mainly) andesine anorthosite complexes of the Central Granulite Terrane, Grenville Province, Quebec: remnants of an older, widespread plutonic event? *Geological Association of Canada/Mineralogical Association of Canada, Program with Abstracts* **23**, 49.

Dymek, R. F. & Owens, B. E. (1998*b*). A belt of late- to post-tectonic anorthosite massifs, Central Granulite Terrane, Grenville Province, Quebec. *Geological Society of America, Abstracts with Program* **30**, 24.

Dymek, R. F. & Schiffries, C. M. (1987). Calcic myrmekite: possible evidence for involvement of water during the evolution of andesine anorthosite from St-Urbain, Quebec. *Canadian Mineralogist* **25**, 291–319.

Emslie, R. F. (1978). Anorthosite massifs, rapakivi granites, and late Proterozoic rifting of North America. *Precambrian Research* **7**, 61–98.

Emslie, R. F. (1980). Geology and petrology of the Harp Lake Complex, Central Labrador: and example of Elsonian magmatism. *Geological Survey of Canada Bulletin* **293**, 136 pp.

Fram, M. S. & Longhi, J. (1992). Phase equilibria of dikes associated with Proterozoic anorthosite complexes. *American Mineralogist* **77**, 605–616.

Frost, B. R., Frost, C. D., Lindsley, D. H., Scoates, J. S. & Mitchell, J. N. (1993). The Laramie anorthosite complex and Sherman batholith: geology, evolution, and theories of origin. In: Snoke, A. W., Steidtmanm, J. R. & Roberts, S. M. (eds) *Geology of Wyoming, Geological Survey of Wyoming Memoir* **5**, 119–161.

Fuhrman, M. L. & Lindsley, D. H. (1988). Ternary feldspar modeling and thermometry. *American Mineralogist* **73**, 201–215.

Fuhrman, M. L., Frost, B. R. & Lindsley, D. H. (1988). Crystallization conditions of the Sybille monzosyenite, Laramie anorthosite complex, Wyoming. *Journal of Petrology* **29**, 699–729.

Goodman, R. J. (1972). The distribution of Ga and Rb in coexisting groundmass and phenocryst phases of some basic volcanic rocks. *Geochimica et Cosmochimica Acta* **36**, 303–317.

Gray, C. M. (1987). Strontium isotopic constraints on the origin of Proterozoic anorthosites. *Precambrian Research* **37**, 173–189.

Green, T. H. (1969). High-pressure experimental studies on the origin of anorthosite. *Canadian Journal of Earth Sciences* **6**, 427–440.

Haskin, L. A., Wildman, T. R. & Haskin, M. A. (1968). An accurate procedure for the determination of the rare earths by neutron activation. *Journal of Radioanalytical Chemistry* **1**, 337–348.

Higgins, M. D. & van Breemen, O. (1992). The age of the Lac-Saint-Jean anorthosite complex and associated mafic rocks, Grenville Province, Canada. *Canadian Journal of Earth Sciences* **29**, 1412–1423.

Higgins, M. D. & van Breemen, O. (1996). Three generations of anorthosite–mangerite–charnockite–granite (AMCG) magmatism, contact metamorphism and tectonism in the Saguenay–Lac-Saint-Jean region of the Grenville Province, Canada. *Precambrian Research* **79**, 327–346.

Hocq, M. (1977). Contribution à la connaissance pétrotectonique et minéralogique des massifs anorthositiques et mangéritiques de la région du réservoir Pipmuacan. Ph.D. thesis, University of Montreal, Montreal, Que.

Kolker, A., Lindsley, D. H. & Hanson, G. N. (1990). Geochemical evolution of the Maloin Ranch pluton, Laramie anorthosite complex, Wyoming: trace elements and petrogenetic models. *American Mineralogist* **75**, 572–588.

Korotev, R. L. (1987*a*). National Bureau of Standards coal flyash (SRM 1633a) as a multielement standard for instrumental neutron activation analysis. *Journal of Radioanalytical and Nuclear Chemistry (Articles)* **110**, 159–177.

Korotev, R. L. (1987*b*). Chemical homogeneity of National Bureau of Standards coal flyash (SRM 1633a). *Journal of Radioanalytical and Nuclear Chemistry (Articles)* **110**, 179–189.

Kranck, E. H. (1961). The tectonic position of the anorthosites of eastern Canada. *Comptes Rendus de la Société Géologique de Finlande* **33**, 300–320.

Lindsley, D. L. & Spencer, K. J. (1982). Fe–Ti oxide geothermometry: reducing analyses of coexisting Ti-magnetite (Mt) and ilmenite (Ilm). *EOS Transactions, American Geophysical Union* **63**, 471.

Liotard, J. M., Vernieres, J. & Dupuy, C. (1979). Variabilité des valeurs de coefficient de partage—influence de la structure des liquides magmatiques. *Chemical Geology* **26**, 237–248.

Longhi, J., Fram, M. S., Vander Auwera, J. & Monteith, J. N. (1993). Pressure effects, kinetics, and rheology of anorthositic and related magmas. *American Mineralogist* **78**, 1016–1030.

Markl, G. & Frost, B. R. (1999). The origin of anorthosites and related rocks from the Lofoten Islands, northern Norway: II. Calculation of parental liquid compositions for anorthosites. *Journal of Petrology* **40**, 61–77.

Martignole, J. & Schrijver, K. (1970). Tectonic setting and evolution of the Morin anorthosite, Grenville Province, Quebec. *Geological Society of Finland Bulletin* **42**, 165–209.

McBirney, A. R. (1979). Effects of assimilation. In: Yoder, H. S. (ed.) *The Evolution of the Igneous Rocks: Fiftieth Anniversary Perspectives*. Princeton, NJ: Princeton University Press, pp. 307–338.

McBirney, A. R. (1989). The Skaergaard layered series: I. Structure and average compositions. *Journal of Petrology* **30**, 363–397.

McLelland, J. M. & Whitney, P. (1990). Anorogenic, bimodal emplacement of anorthositic, charnockitic and related rocks in the Adirondack Mountains, New York. In: Stein, H. J. & Hannah, J. L. (eds) *Ore-bearing Granite Systems; Petrogenesis and Mineralizing Processes. Geological Society of America, Special Papers* **246**, 301–315.

Mitchell, J. N., Scoates, J. S. & Frost, C. D. (1996). High-Al gabbros in the Laramie anorthosite complex, Wyoming: implications for the composition of melts parental to Proterozoic anorthosite. *Contributions to Mineralogy and Petrology* **119**, 166–180.

Morin, M. (1969). Labrieville area, Saguenay County. *Quebec Department of Natural Resources Geological Report* **141**, 45 pp.

Morse, S. A. (1980). *Basalts and Phase Diagrams*. New York: Springer, 493 pp.

Morse, S. A. (1981). Kiglapait geochemistry IV: the major elements. *Geochimica et Cosmochimica Acta* **45**, 461–479.

Morse, S. A. (1982*a*). Kiglapait geochemistry V: strontium. *Geochimica et Cosmochimica Acta* **46**, 223–234.

Morse, S. A. (1982*b*). A partisan review of Proterozoic anorthosites. *American Mineralogist* **67**, 1087–1100.

Morse, S. A. (1992). Partitioning of strontium between plagioclase and melt: a comment. *Geochimica et Cosmochimica Acta* **56**, 1735–1737.

Morse, S. A. & Nolan, K. M. (1984). Origin of strongly reversed rims on plagioclase in cumulates. *Earth and Planetary Science Letters* **68**, 485–498.

Owens, B. E. (1998). Late-Grenvillian lamprophyres in the Labrieville massif, Quebec: clues to the source characteristics of alkalic anorthosites? *Geological Society of America, Abstracts with Program* **30**, 24.

Owens, B. E. & Dymek, R. F. (1992). Fe-, Ti- and P-rich rocks and massif anorthosite: problems of interpretation illustrated from the Labrieville and St-Urbain plutons, Quebec. *Canadian Mineralogist* **30**, 163–190.

Owens, B. E. & Dymek, R. F. (1995). Significance of pyroxene megacrysts for massif anorthosite petrogenesis: constraints from the Labrieville, Quebec, pluton. *American Mineralogist* **80**, 144–161.

Owens, B. E. & Dymek, R. F. (1998). A 'newly' recognized andesine anorthosite in the Grenville Province: recent observations on the Mattawa massif, Lac-Saint-Jean region, Quebec. *Geological Association of Canada/Mineralogical Association of Canada, Program with Abstracts* **23**, 139.

Owens, B. E. & Dymek, R. F. (1999*a*). A geochemical reconnaissance of the Roseland anorthosite complex, Virginia, and comparisons with andesine anorthosites from the Grenville Province of Quebec. In: Sinha, A. K. (ed.) *Basement Tectonics: Proceedings of the 13th International Conference on Basement Tectonics*. Dordrecht, Kluwer Academic, pp. 217–232.

Owens, B. E. & Dymek, R. F. (1999b). Concentrically zoned andesine anorthosites in the Grenville Province of Quebec. *Geological Society of America, Abstracts with Program* **31**, 415.

Owens, B. E., Rockow, M. W. & Dymek, R. F. (1993). Jotunites from the Grenville Province, Quebec: petrological characteristics and implications for massif anorthosite petrogenesis. *Lithos* **30**, 57–80.

Owens, B. E., Dymek, R. F., Tucker, R. D., Brannon, J. C. & Podosek, F. A. (1994). Age and radiogenic isotopic composition of a late- to post-tectonic anorthosite in the Grenville Province: the Labrieville massif, Quebec. *Lithos* **31**, 189–206.

Ranson, W. A. (1981). Anorthosites of diverse magma types in the Puttuaaluk Lake area, Nain Complex, Labrador. *Canadian Journal of Earth Sciences* **18**, 26–41.

Rivers, T., Martignole, J., Gower, C. F. & Davidson, A. (1989). New tectonic divisions of the Grenville Province, southeast Canadian Shield. *Tectonics* **8**, 63–84.

Salpas, P. A., Haskin, L. A. & McCallum, I. S. (1983). Stillwater anorthosites: a lunar analog? *Proceedings of the 14th Lunar and Planetary Science Conference. Journal of Geophysical Research* **88**(supplement), 27–39.

Schiellerup, H., Lambert, D. D., Prestvik, T., Robins, B., McBride, J. & Larsen, R. B. (2000). Re–Os isotopic evidence for a lower crustal origin of massif anorthosites. *Nature* **405**, 781–784.

Scoates, J. S. (2000). The plagioclase-magma density paradox re-examined and the crystallization of Proterozoic anorthosites. *Journal of Petrology* **41**, 627–649.

Scoates, J. S. & Mitchell, J. N. (2000). The evolution of troctolitic and high Al basaltic magmas in Proterozoic anorthosite plutonic suites and implications for the Voisey's Bay massive Ni–Cu sulfide deposit. *Economic Geology* **95**, 677–701.

Scoates, J. S., Frost, C. D., Mitchell, J. N., Lindsley, D. H. & Frost, B. R. (1996). Residual-liquid origin for a monzonite intrusion in a mid-Proterozoic anorthosite complex: the Sybille intrusion, Laramie

anorthosite complex, Wyoming. *Geological Society of America Bulletin* **108**, 1357–1371.

Simmons, E. C. & Hanson, G. N. (1978). Geochemistry and origin of massif anorthosite. *Contributions to Mineralogy and Petrology* **66**, 119–135.

Sisson, T. W. & Grove, T. L. (1993). Experimental investigations of the role of H_2O in calc-alkaline differentiation and subduction zone magmatism. *Contributions to Mineralogy and Petrology* **113**, 143–166.

Spencer, K. J. & Lindsley, D. H. (1981). A solution model for coexisting iron–titanium oxides. *American Mineralogist* **66**, 1189–1201.

Tsuchiyama, A. (1985). Dissolution kinetics of plagioclase in the melt of the system diopside–albite–anorthite, and origin of dusty plagioclase in andesites. *Contributions to Mineralogy and Petrology* **89**, 1–16.

Vander Auwera, J. & Longhi, J. (1994). Experimental study of a jotunite (hypersthene monzodiorite): constraints on the parent magma composition and crystallization conditions of the Bjerkreim–Sokndal layered intrusion (Norway). *Contributions to Mineralogy and Petrology* **118**, 60–78.

Vander Auwera, J., Longhi, J. & Duchesne, J. C. (1998). A liquid line of descent of the jotunitic (hypersthene monzodiorite) suite. *Journal of Petrology* **39**, 439–468.

Vander Auwera, J., Longhi, J. & Duchesne, J. C. (2000). The effect of pressure on D_{Sr} (plag/melt) and D_{Cr} (opx/melt): implications for anorthosite petrogenesis. *Earth and Planetary Science Letters* **178**, 303–314.

Wager, L. R. & Brown, G. M. (1967). *Layered Igneous Rocks*. San Francisco, CA: W. H. Freeman, 588 pp.

Windley, B. F. (1989). Anorogenic magmatism and the Grenvillian Orogeny. *Canadian Journal of Earth Sciences* **26**, 479–489.

Woussen, G., Roy, D. W., Dimroth, E. & Chown, E. H. (1986). Mid-Proterozoic extensional tectonics in the core zone of the Grenville Province. In: Moore, J. M., Davidson, A. & Baer, A. J. (eds) *The Grenville Province. Geological Association of Canada Special Paper* **31**, 297–311.

Woussen, G., Martignole, J. & Nantel, S. (1988). The Lac-St-Jean anorthosite in the St-Henri-de-Taillon area (Grenville Province): a relic of a layered complex. *Canadian Mineralogist* **26**, 1013–1025.

Wynne-Edwards, H. R. (1972). The Grenville Province. In: Price, R. A. & Douglas, R. J. W. (eds) *Variations in Tectonic Styles in Canada. Geological Association of Canada, Special Paper* **11**, 263–334.

Yoder, H. S., Jr (1969). Calcalkalic andesites: experimental evidence bearing on the origin of their assumed characteristics. In: McBirney, A. R. (ed.) *Proceedings of the Andesite Conference. Oregon Department of Geology and Mineral Industries Bulletin* **65**, 77–89.

Xue, S. & Morse, S. A. (1993). Geochemistry of the Nain anorthosite, Labrador: magma diversity in five intrusions. *Geochimica et Cosmochimica Acta* **57**, 3925–3948.

APPENDIX: ANALYTICAL METHODS

All whole-rock chemical compositions presented in this paper represent XRF analyses carried out at Washington University using an automated Siemens SRS-200 instrument. Concentrations of major and minor elements were obtained by analysis of fused glass disks using methods described by Couture *et al.* (1993); trace element concentrations were obtained by analysis of pressed-powder pellets using combined Compton and fundamental parameters methods described by Couture & Dymek (1996). Selected trace elements were determined in a subset of samples by INAA, also at Washington University, using methods described by Korotev (1987*a*, 1987*b*). Trace elements determined by XRF include V, Cr, Co, Ni, Cu, Zn, Ga, Rb, Sr, Y, Zr, Nb, Ba, and Pb. Trace elements determined by INAA include Sc, Cr, Co, Ni, As, Br, Sb, Rb, Sr, Zr, Cs, Ba, La, Ce, Sm, Eu, Tb, Yb, Lu, Hf, Ta, W, Th, U, and Au. In the case where two methods determined the same elements, the data reported in the tables correspond to the more precise method in each case: XRF for Sr, Ba, Rb, and Ni; and INAA for Cr and Co.

All mineral compositions reported in this paper represent EMP analyses carried out at Washington University using an automated JEOL-733 instrument. Operating conditions were 15 kV accelerating potential, 20 nA beam current, 1–20 μm spot size, and counting times of 10–100 s (the spot size and counting times were adjusted according to element and mineral being analyzed). Simple silicates and oxides were used as primary standards [Na—albite; Mg,Si—enstatite; Al—kyanite, Ca—wollastonite; Ca,Al—anorthite (synthetic); K—microcline; Ti—rutile; Cr—eskolaite (synthetic); Mn—rhodonite; Fe—fayalite (synthetic); Ba—celsian (synthetic)]. X-ray intensities were converted to oxide weight percent following the methods of Bence & Albee (1968), with correction factors modified from those listed by Albee & Ray (1970). Errors are judged to be $\sim 1\%$ relative for most oxides based on repetitive analysis of working standards (Kakanui augite and Nain labradorite) during the course of each run.